NAVAL POSTGRADUATE SCHOOL

MONTEREY, CALIFORNIA

THESIS

LOW SPECTRAL EFFICIENCY TRELLIS CODED MODULATION SYSTEMS

by

Konstantinos Pyloudis

September 2006

Thesis Advisor:	Clark Robertson
Thesis Co Advisor:	Tri Ha

Approved for public release; distribution is unlimited

THIS PAGE INTENTIONALLY LEFT BLANK

REPORT DOCUMENTATION PAGE			Form Approved OMB No. 0704-0188
Public reporting burden for this collection of information is estimated to average 1 hour per response, including the time for reviewing instruction, searching existing data sources, gathering and maintaining the data needed, and completing and reviewing the collection of information. Send comments regarding this burden estimate or any other aspect of this collection of information, including suggestions for reducing this burden, to Washington headquarters Services, Directorate for Information Operations and Reports, 1215 Jefferson Davis Highway, Suite 1204, Arlington, VA 22202-4302, and to the Office of Management and Budget, Paperwork Reduction Project (0704-0188) Washington DC 20503.			
1. AGENCY USE ONLY *(Leave blank)*	**2. REPORT DATE** September 2006	**3. REPORT TYPE AND DATES COVERED** Master's Thesis	
4. TITLE AND SUBTITLE: Low Spectral Efficiency Trellis Coded Modulation Systems			**5. FUNDING NUMBERS**
6. AUTHOR Konstantinos Pyloudis			
7. PERFORMING ORGANIZATION NAME(S) AND ADDRESS(ES) Naval Postgraduate School Monterey, CA 93943-5000			**8. PERFORMING ORGANIZATION REPORT NUMBER**
9. SPONSORING /MONITORING AGENCY NAME(S) AND ADDRESS(ES) N/A			**10. SPONSORING/MONITORING AGENCY REPORT NUMBER**
11. SUPPLEMENTARY NOTES The views expressed in this thesis are those of the author and do not reflect the official policy or position of the Department of Defense or the U.S. Government.			
12a. DISTRIBUTION / AVAILABILITY STATEMENT Approved for public release; distribution is unlimited			**12b. DISTRIBUTION CODE**

13. ABSTRACT (maximum 200 words)

Trellis-coded modulation (TCM) is a known technique to increase the data rate without increasing the channel bandwidth when implementing error correction coding. TCM is a combination of *M-ary* modulation and error correction coding. This thesis investigates the performance of a low spectral efficiency TCM system, which is compared with three alternative systems having comparable bandwidth. The three alternative systems are all non-TCM systems and consist of QPSK with independent r=1/2 error correction coding on the in-phase and quadrature components, *8-ary* biorthogonal keying (*8-BOK*) with r=2/3 error correction coding, and 16-BOK with r=3/4 error correction coding. The effects of both additive white Gaussian noise (AWGN) and pulse-noise interference (PNI) are considered. The TCM system shows mush better than expected performance and significant resistance to PNI, and performance improves as the number of memory element increases. The alternative QPSK system with soft decision decoding (SDD) experiences significant degradation with PNI. The 8-BOK with r=2/3 error correction and 16-BOK with r=3/4 error correction systems occupy approximately the same bandwidth as the TCM system and show better performance in PNI than the alternative QPSK system.

14. SUBJECT TERMS TCM, Trellis Coded Modulation, Hard decision decoding, Soft decision deciding, pulse-noise interference, BER, Set partition, M-BOK, QPSK, AWGN			**15. NUMBER OF PAGES** 101
			16. PRICE CODE
17. SECURITY CLASSIFICATION OF REPORT Unclassified	**18. SECURITY CLASSIFICATION OF THIS PAGE** Unclassified	**19. SECURITY CLASSIFICATION OF ABSTRACT** Unclassified	**20. LIMITATION OF ABSTRACT** UL

NSN 7540-01-280-5500 Standard Form 298 (Rev. 2-89)
Prescribed by ANSI Std. 239-18

THIS PAGE INTENTIONALLY LEFT BLANK

Approved for public release; distribution is unlimited

LOW SPECTRAL EFFICIENCY TRELLIS CODED MODULATION SYSTEMS

Konstantinos Pyloudis
Captain, Hellenic Air Force
Bachelor of Engineering, Hellenic Air Force Academy (Electrical Engineering Department), 1994

Submitted in partial fulfillment of the
requirements for the degree of

MASTER OF SCIENCE IN SYSTEMS ENGINEERING
and
MASTER OF SCIENCE IN ELECTRICAL ENGINEERING

from the

NAVAL POSTGRADUATE SCHOOL
September 2006

Author: Konstantinos Pyloudis

Approved by: Clark Robertson
Thesis Advisor

Tri Ha
Co-Advisor

Jeffrey Knorr
Chairman, Department of Electrical and Computer Engineering

Dan C. Boger
Chairman, Department of Information Sciences

THIS PAGE INTENTIONALLY LEFT BLANK

ABSTRACT

Trellis-coded modulation (TCM) is a known technique to increase the data rate without increasing the channel bandwidth when implementing error correction coding. TCM is a combination of *M-ary* modulation and error correction coding. This thesis investigates the performance of a low spectral efficiency TCM system, which is compared with three alternative systems having comparable bandwidth. The three alternative systems are all non-TCM systems and consist of QPSK with independent $r=1/2$ error correction coding on the in-phase and quadrature components, *8-ary* biorthogonal keying (*8-BOK*) with $r=2/3$ error correction coding, and 16-BOK with $r=3/4$ error correction coding. The effects of both additive white Gaussian noise (AWGN) and pulse-noise interference (PNI) are considered. The TCM system shows much better than expected performance and significant resistance to PNI, and performance improves as the number of memory element increases. The alternative QPSK system with soft decision decoding (SDD) experiences significant degradation with PNI. The 8-BOK with $r=2/3$ error correction and 16-BOK with $r=3/4$ error correction systems occupy approximately the same bandwidth as the TCM system and show better performance in PNI than the alternative QPSK system.

THIS PAGE INTENTIONALLY LEFT BLANK

TABLE OF CONTENTS

THIS PAGE INTENTIONALLY LEFT BLANK

LIST OF FIGURES

LIST OF TABLES

THIS PAGE INTENTIONALLY LEFT BLANK

ACKNOWLEDGMENTS

The author is sincerely grateful to his thesis advisor Professor R. Clark Robertson. Without his constant advice, guidance, encouragement, and support, this thesis would not have been possible.

The author would also like to acknowledge the initial ideas and guidance he received from Professor Tri Ha.

The author also thanks his country, Greece, and the Hellenic Air Force for providing him with the opportunity to study at the Naval Postgraduate School.

Finally, the author would like to thank his wife, Maria, for her understanding, tireless patience, and unfailing support. This thesis is dedicated to her, to my son Christos, my daughter, Ioanna, and to our unborn baby.

THIS PAGE INTENTIONALLY LEFT BLANK

EXECUTIVE SUMMARY

The goal of this thesis was to investigate the performance of a low spectral efficiency trellis-coded modulation (TCM) system with QPSK modulation and r=1/2 correction coding. TCM is a known technique to increase the data rate without increasing the channel bandwidth when implementing error correction coding. This has been achieved with set partitioning which was introduced by Ungerboeck [1] and was described as "the key that cracked the problem of constructing efficient coded modulation techniques for band limited channels." TCM is a combination of *M-ary* modulation and error correction coding.

In this thesis the performance of a low spectral efficiency TCM system is compared with three alternative systems having comparable bandwidth. The occupied bandwidth for the TCM system is $BW = 2R_b$. The three alternative systems are all non-TCM systems and consist of QPSK with independent r=1/2 error correction coding on the in-phase and quadrature components, with null-to-null bandwidth $BW = 2R_b$, 8-*ary* biorthogonal keying (*8-BOK*) with r=2/3 error correction coding with bandwidth $BW = 21/12\, R_b$ and 16-BOK with r=3/4 error correction coding and with bandwidth $BW = 44/24\, R_b$.

At the beginning of the analysis only the effect of additive white Gaussian noise (AWGN)) is considered. The performance of the TCM system with QPSK modulation and r=1/2 error correction coding is identical to the performance of QPSK with independent r=1/2 error correction coding on the in-phase and quadrature components. 8-BOK with r=2/3 error correction coding and 16-BOK with r=3/4 error correction coding performs poorly compared with the TCM system, with the second (16-BOK with r=3/4 error correction) having better performance than the first (8-BOK with r=2/3 error correction coding).

The effect of pulse-noise interference (PNI) is then considered for all four systems. With the addition of pulse-noise interference, things change dramatically. The TCM system shows much better than expected performance and significant resistance to

PNI, and performance improves as the number of memory element increases. The alternative QPSK system with soft decision decoding (SDD) and linear combining experiences significant degradation with PNI, showing no immunity at all in a pulse-noise interference environment. The 8-BOK with r=2/3 error correction and 16-BOK with r=3/4 error correction systems show better performance in PNI than the alternative QPSK system but much worse compared to the TCM system. It is noteworthy that 16-BOK with r=3/4 error correction coding, which had better performance than 8-BOK with r=2/3 error correction coding in AWGN, in a pulse-noise interference environment experiences significant degradation and much worse performance as compared with 8-BOK with r=2/3 correction coding.

I. INTRODUCTION

A. OBJECTIVES

Modern communication systems require reliable communications, with high speed data rates and maximum throughput. Moreover, it is of great importance to minimize the required bandwidth and the required power. Everyone wants to communicate with high speed data rates and be able to transfer files and video data without delays in a robust communication system.

Although error correction coding improves reliability by adding redundant bits and improving the bit error ratio, its drawback is the resulting bandwidth expansion. Especially for a band limited system such as a telephone line, the use of error correction coding is difficult due to the increased required bandwidth.

With the introduction of Trellis-coded modulation (TCM), channel coding is possible without an increase in bandwidth. In this thesis, the performance of a TCM system for low spectral efficiencies will be investigated and compared with several non-TCM systems having comparable spectral efficiencies.

B. RELATED RESEARCH

For many years the use coding in a band limited channel has been great area of interest. Ungerboeck, in 1982, showed that coding gains are achievable, using the principle of *mapping by set partitioning* [1,2,4], without increasing channel bandwidth. This technique is called trellis-coded modulation.

In this thesis the performance of TCM with QPSK modulation is compared with that of ordinary convolutional encoders with QPSK modulation, designed such that the data rate and bandwidth are the same for both systems. Two comparisons are made. First, the two systems are assumed to have the same number of memory elements devoted to overall encoding. In other words, if the TCM encoder has K memory elements, then each of the ordinary convolutional encoders in the alternative system will have $K/2$ memory elements for a total of K memory elements. Second, if the TCM encoder has K memory elements, then each of the ordinary convolutional encoders in the

alternative system has K memory elements for a total of $2K$ memory elements. In addition, 8-BOK with r=2/3 convolutional coding and 16-BOK with r=3/4 convolutional coding are also considered since they have almost the same spectral efficiency as the TCM system under consideration.

Since military systems must operate in hostile environments, this thesis also investigates the performance of the four systems when pulse-noise interference (PNI) is present in addition to additive white Gaussian noise (AWGN). To the best of the author's, knowledge there is no related research involving TCM with pulse-noise interference.

C. OUTLINE

This thesis is organized into five remaining chapters after the introduction. Chapter II is a review of TCM and an explanation of basic ideas such as set partitioning, squared Euclidean distance, trellis encoder, and bit error probability of TCM. In Chapter III, the performance of the TCM system in AWGN is analyzed and compared with the performance of the alternative systems in AWGN. Chapter IV examines the effect of pulse-noise interference on the TCM system. An interesting result is that the immunity of the TCM system to PNI is significant and the degradation that the alternative QPSK system has is marked. In Chapter V, 8-BOK with r=2/3 convolutional coding and 16-BOK with r=2/3 convolutional coding are presented as alternative systems that occupy almost the same bandwidth as the QPSK TCM system. Both 8-BOK and 16-BOK are exposed to pulse-noise interference where the same immunity is absent that is found with TCM. Finally, in Chapter VI some conclusions are made based on the results obtained from the previous chapters. Also, recommendations for future research are proposed.

II. TCM BACKGROUND

A. WHY TCM

In a digital communication system, coding is used in order to increase the immunity of the system to noise. In such a way, the robustness of the communication system is increased. The penalty is the expansion in required bandwidth. Trellis coded modulation is a method that combines error correction coding and non-binary modulation techniques in such a way that data rate can be increased without increasing the channel bandwidth. In a bandwidth limited environment, this is an efficient method to increase the robustness of the system.

1. TCM Theory

An example described in [4] is a good way to understand the concept of TCM. In Figure 1 there are three different digital communication schemes transmitting two information bits every T seconds. In Figure 1a is QPSK modulation without coding and with one signal every T seconds. Here every signal carries two information bits. In Figure 1b, a convolutional encoder with rate r=2/3 and QPSK modulation is used. Now every signal carries an average of 4/3 information bits and must have a duration of 2T/3 in order to match the information rate of the uncoded system in Figure 1a. This implies a bandwidth expansion of 3/2 *(50%)* compared with the first case. Finally, in the communication scheme shown in Figure 1c, an r=2/3 convolutional encoder is used with 8-PSK modulation. Now no reduction in the signal duration is required to maintain the same data rate as the system depicted in Figure 1a. Two information bits are carried by each signal, and there is no bandwidth expansion because 8-PSK and 4-PSK occupy the same bandwidth given the same symbol rate.

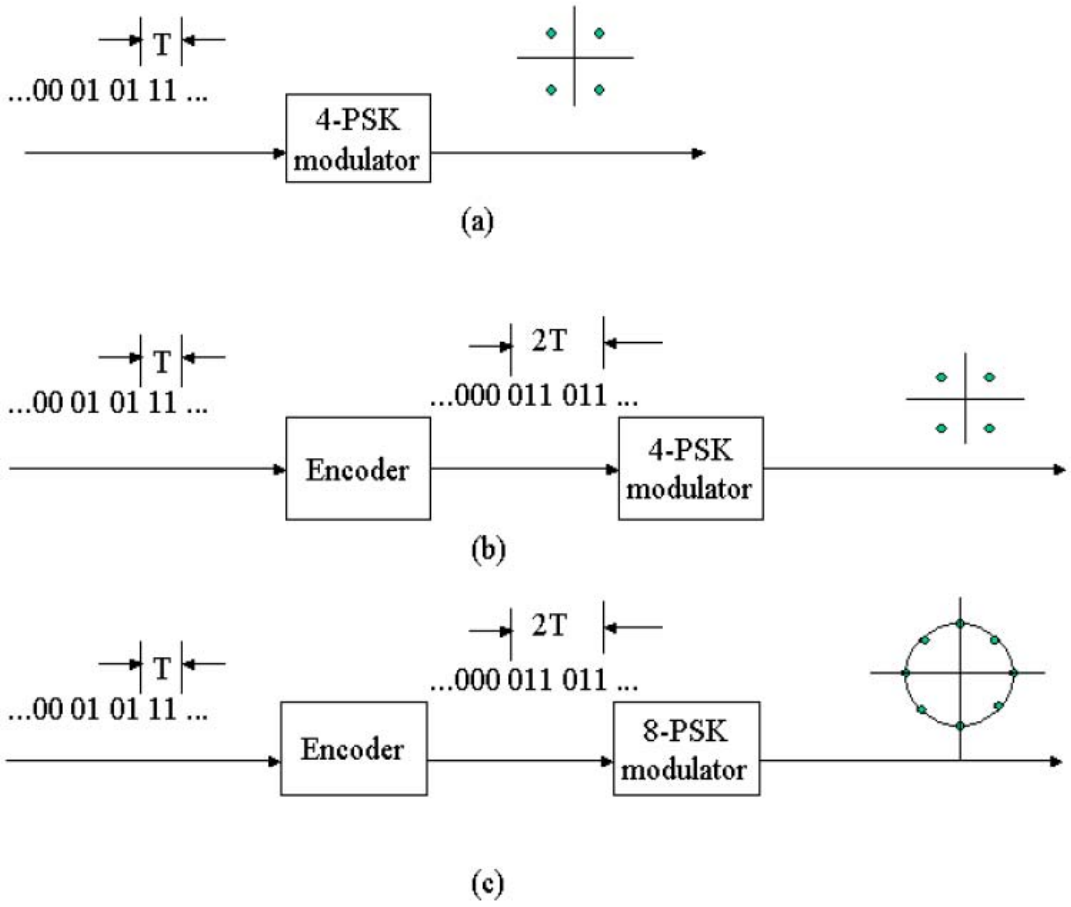

Figure 1. Three digital communication schemes transmitting two information bits every T seconds: (a) uncoded transmission with QPSK (b) QPSK with a rate 2/3 convolutional encoder and bandwidth expansion (c) 8-PSK with a rate 2/3 convolutional encoder and no bandwidth expansion. From [4]

It can be seen that with the communication scheme depicted in Figure 1c there is coding and no bandwidth expansion. This is the concept of TCM. Encoding and modulation are not treated independently but together as one operation. With TCM it can be said that there is no bandwidth expansion but signal set expansion. For conventional systems with convolutional codes, the free Hamming distance is an important figure of merit, but with TCM the free Euclidean distance between signal points is more important. Generally, the choices of coding and signal constellation do not take place separately.

2. Set Partitioning

Returning to the example in Figure 1a, we see that two bits per time T (symbol time) are transmitted, making QPSK the logical modulation. In Figure 1(c) 8-PSK modulation is chosen since each symbol has three bits. Choosing 8-PSK avoids any bandwidth increase over QPSK since the symbol rate is unchanged. From Figure 2 it can be seen that 8-PSK can be partitioned into two sets of four symbols, and each of these sets can be partitioned into two sets of two symbols. From the initial 8-PSK set, there are four sets of two symbols each that are referred to as subsets.

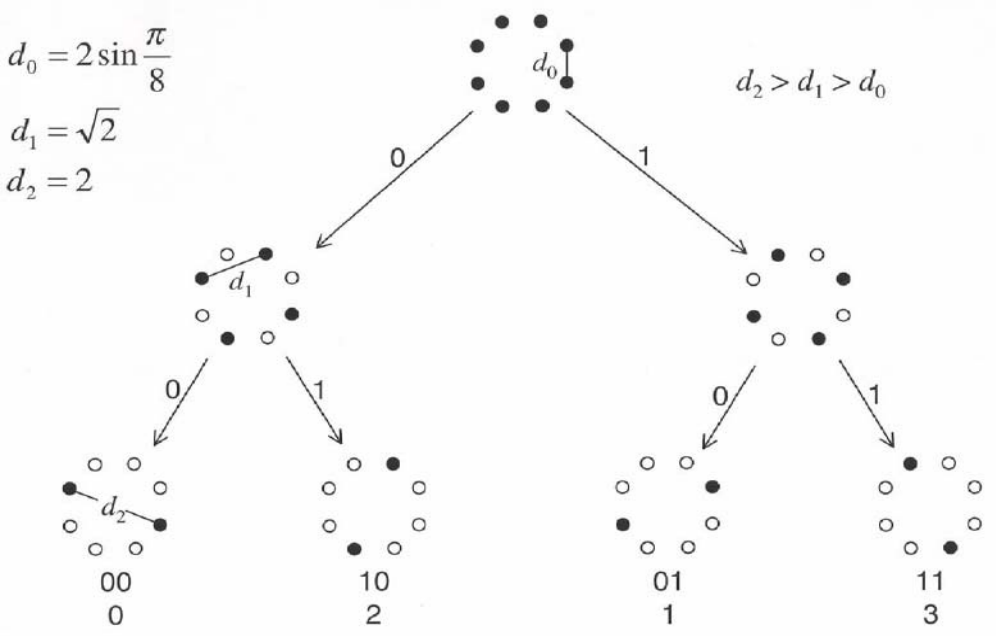

Figure 2. Partitioning of 8-PSK constellation. From [5]

What has been achieved with the set partitioning is smaller signal constellations. Also, the Euclidean distances between the signal points in a set have been maximized. Set partitioning was introduced by Ungerboeck [1] and was described as “the key that cracked the problem of constructing efficient coded modulation techniques for band limited channels.”

B. TCM ENCODER

1. Encoder for 8-PSK

After the set partitioning of 8-PSK, the encoder shown in Figure 3 can be used. Since there are two information bits per time T (symbol time), one bit will be applied to the convolutional encoder. From the encoder output one of the signal sets is chosen. The uncoded bit selects a signal from the subset to be transmitted.

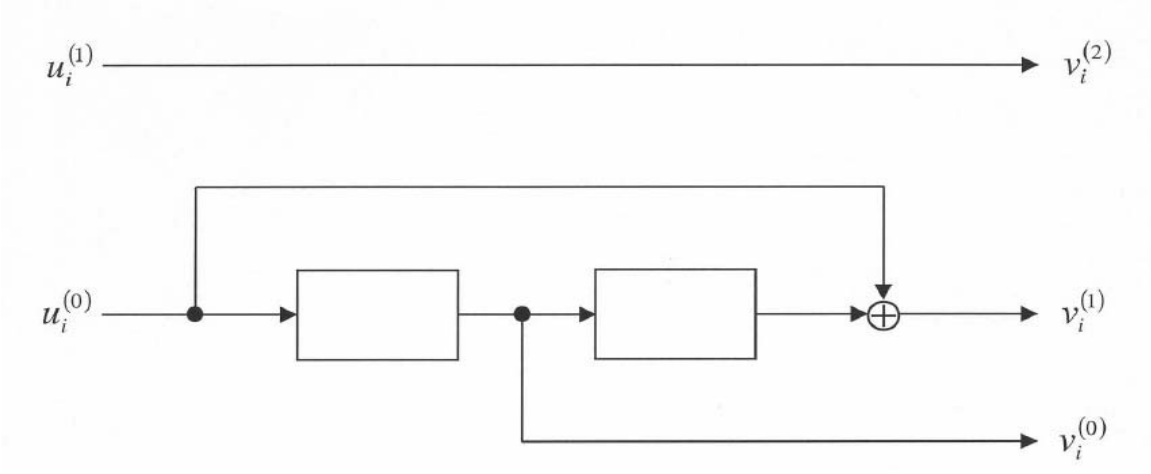

Figure 3. TCM encoder with a single parallel transition/branch for 8-ary signaling. From [5]

2. Parallel Transitions

In Figure 3 a rate r=1/2 convolutional encoder was used, so the output can be described by a trellis diagram. The difference from the conventional trellis diagram is that with the r=1/2 convolutional encoder there are two possible branch transitions depending on the uncoded bit. The extra transitions are called *parallel transitions.* Parallel transitions with 8-PSK can be eliminated if a code rate r=2/3 convolutional code is used, such as the one shown in Figure 4.

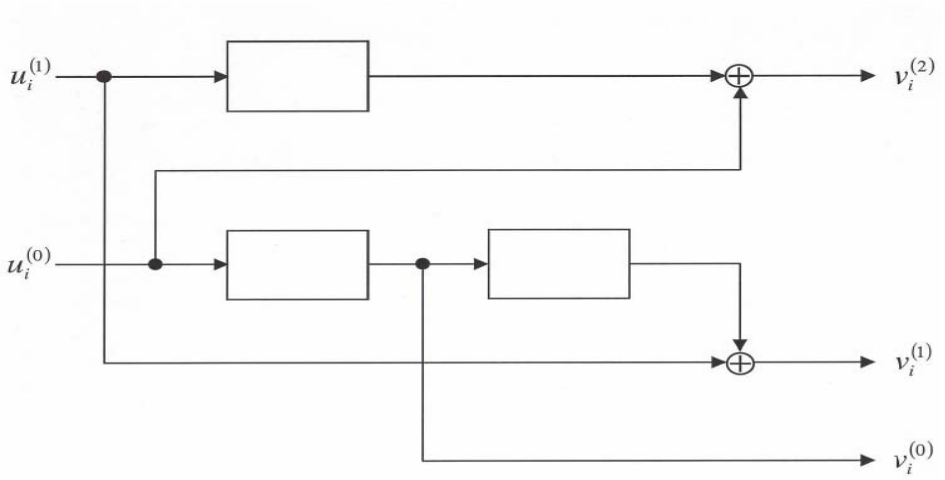

Figure 4. TCM encoder with no parallel transitions/branch for 8-ary signaling. From [5]

The trellis diagram for the TCM encoder with one parallel transition for 8-ary signaling is shown in Figure 5.

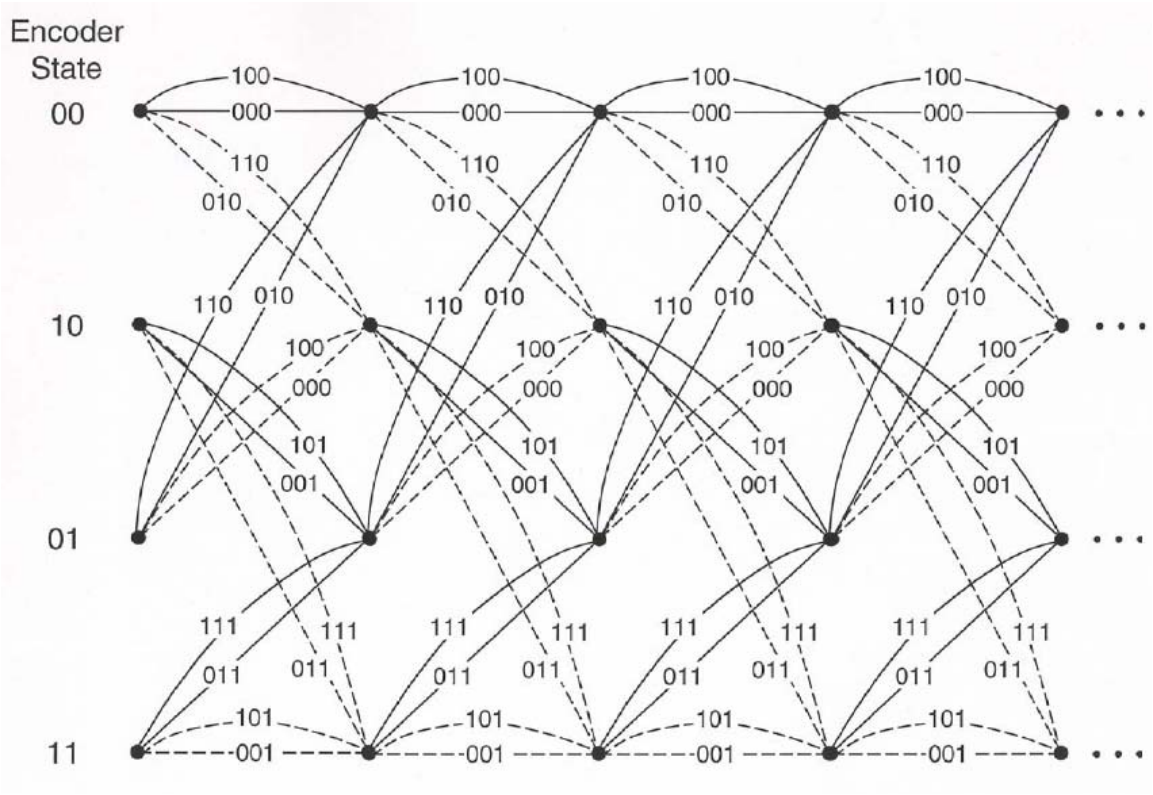

Figure 5. Trellis diagram for TCM encoder with a single parallel transition/branch for 8-ary signaling. From [5]

3. TCM Encoder

The previous sections examined the case of 8-PSK. It was desired to transmit two bits per symbol duration T and 8-PSK was used in order to avoid bandwidth expansion. Of course, 8-QAM can also be used. Generalizing the theory introduced by Ungerboeck [1], whenever m bits per symbol time are to be transmitted, instead of using 2^m - QAM or 2^m-PSK, 2^{m+1}-QAM or 2^{m+1}-PSK is used and the constellation can be partitioned in order to implement TCM. Depending on the convolutional encoder used, various numbers of parallel transitions can occur. If an encoder is selected with code rate $r=1/2$, then one information bit will be applied to the encoder that will choose one of the subsets from the second partition level, each one containing 2^{m-1} symbols. The remaining m-1 uncoded bits will select a signal from the selected subset.

The number of parallel transitions in this case will be 2^{m-1}-1. Continuing the process with a $r=2/3$ convolutional encoder, we see that two information bits are applied to the encoder and at the output they choose one of the subsets at the third partition level, each one containing 2^{m-2} symbols. The remaining m-2 uncoded bits will select a signal from the selected subset. The number of parallel transitions in this case will be 2^{m-1}-2. If all the m information bits are applied to an $r=m/m+1$ convolutional encoder, then there will be no parallel transitions. In many cases this is the objective, but the disadvantage is that by increasing m the complexity of the $r=m/m+1$ convolutional encoder is also increased. In Figure 6, the general structure of a TCM encoder is shown.

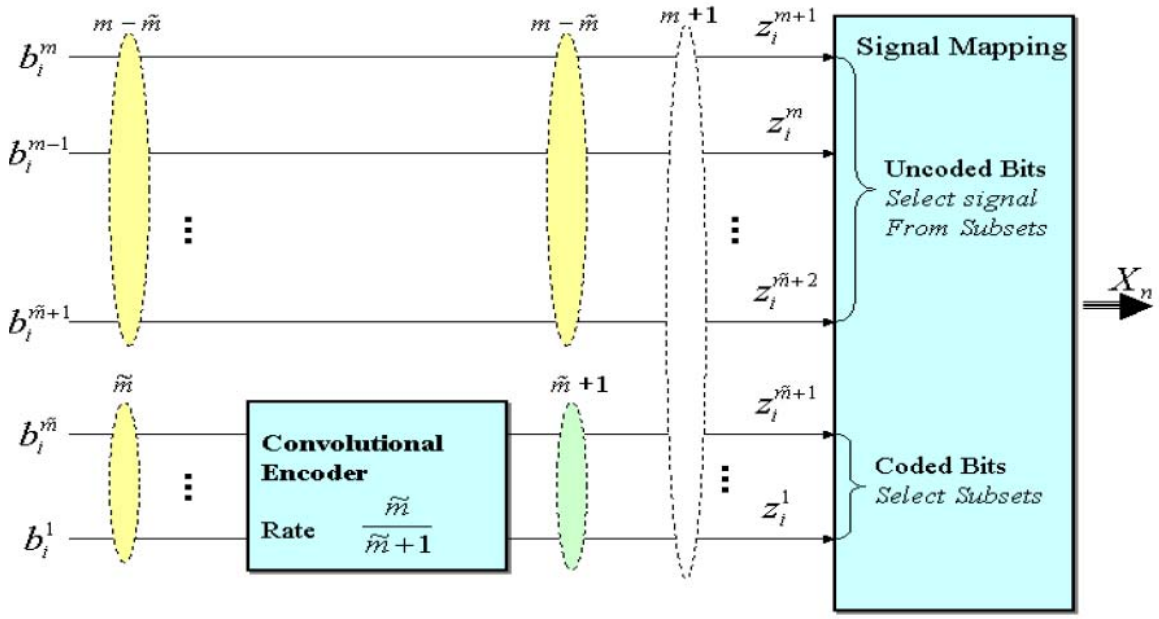

Figure 6. Block diagram of an Ungerboeck encoder. After [3]

C. TCM PERFORMANCE

1. Performance

The performance of TCM systems can be analyzed by obtaining the *average input output enumerating function* (AIOWEF) $T_{ave}(X,Y)$ [5]. First, the *error trellis* of the convolutional code must be obtained. Distance properties of the TCM system can be analyzed through the trellis diagram in a way similar to that for conventional convolutional codes. The Viterbi algorithm is used for decoding. The Viterbi algorithm decodes the convolutional code by selecting the most likely path through the trellis, which represents the received code sequence and is associated with a given received information sequence. The Viterbi algorithm requires the definition of path metrics. The algorithm searches all the paths in the trellis diagram and selects the path that has the best metric. The difference between a conventional trellis and an *error trellis* is that with the conventional trellis each branch is equivalent to the encoder output corresponding to that specific transition [5]. On the other hand, with the error trellis each branch is equivalent to the *error vector* corresponding to that specific transition [5]. As stated in [5], the error vector of code sequence **v** and code sequence **v´** is defined as $\mathbf{e(v, v')} = \mathbf{v} \oplus \mathbf{v'}$. Without loss of generality $\mathbf{v'=0}$ can be chosen, since the convolutional code is linear. Now $\boldsymbol{e=v}$,

and the conventional trellis is identical to the error trellis. The difference is in the interpretation. In order to obtain the AIOWEF, the state diagram is first converted into a signal flow graph. In conventional codes each branch of the signal flow graph is labeled with X^dY^JZ where X^dY^JZ is the branch gain, *d* is the weight of the encoder output for that branch, *j* is the information weight, and Z corresponds to the input bits. By replacing X^dY^JZ with $\Delta^2_e(X)\ Y^JZ$ and using the transfer function of the signal flow graph, we obtain the AIOWEF. $\Delta^2_e(X)$ is the *average Euclidean weight enumerator* (AEWE), which is the average of the squared-Euclidean distance enumerating functions between all pairs of signal points in the constellation having the same error vector and is given by

$$\Delta_e^2(X) = \frac{1}{M}\sum_{v} X^{\Delta_v^2(e)} \tag{2.1}$$

where M is the number of sequences and $\Delta_v^2(e)$ is the squared-Euclidean distances between **v** and some arbitrary reference **v´** [5].

The best way to understand the concept is with an example given in [5] with QPSK modulation, the modulation scheme examined in this thesis. The convolutional encoder that will be used has code rate r=1/2 and constrain length v=3. QPSK is considered with Gray mapping as shown in Figure 7.

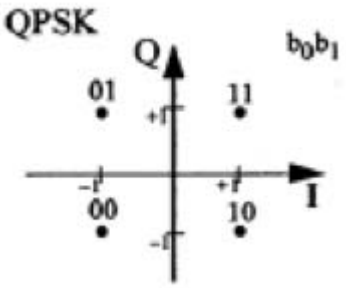

Figure 7. QPSK Constellation plot. From [2]

For Gray mapping it is obvious, as stated in [5], that ***e(00, 01)=e(11, 10)=01*** and as a result

$$\Delta_{01}^2(X) = \frac{1}{2}X^2 + \frac{1}{2}X^2 = X^2$$

In the same way ***e(00 , 11)=e(01, 10)=11***, and

$$\Delta_{11}^{2}(X) = \frac{1}{2}X^{4} + \frac{1}{2}X^{4} = X^{4}$$

Similarly, ***e(00 , 11)=e(01, 10)=11***, and

$$\Delta_{10}^{2}(X) = \frac{1}{2}X^{2} + \frac{1}{2}X^{2} = X^{2}$$

Finally, ***e(00 , 00)=e(11, 11)= e(01 , 01)=e(10, 10)=00*** ,and

$$\Delta_{00}^{2}(X) = \frac{1}{2}X^{0} + \frac{1}{2}X^{0} = 1$$

The signal flow graph for the rate r=1/2 and constrain length v=3 convolutional encoder in Figure 8, with QPSK/TCM, is shown in Figure 9 and is obtained by replacing X with X^2 on the conventional signal flow graph. The transfer function of the conventional convolutional code is $T(X,Y)=X^5Y(1-2XY)^{-1}$. Now $T_{ave}(X,Y)=T(X^2,Y)$, and the AIOWEF is $T_{ave}(X,Y)=X^{10}Y(1-2X^2Y)^{-1}$ [5]. From the geometric series

$$\frac{1}{1-r} = 1 + r + r^2 + r^3 + r^4 + r^5 + ... \qquad (2.2)$$

$T_{ave}(X,Y)=X^{10}Y(1+2X^2Y+4X^4Y^2 +8\ X^6Y^3 +.....)$. The AIOWEF implies that there is one code sequence with a squared-Euclidean distance of ten. Moreover, the AIOWEF implies that there are two code sequences with squared-Euclidean distances of twelve, four code sequences with squared-Euclidean distances of fourteen, and so on.

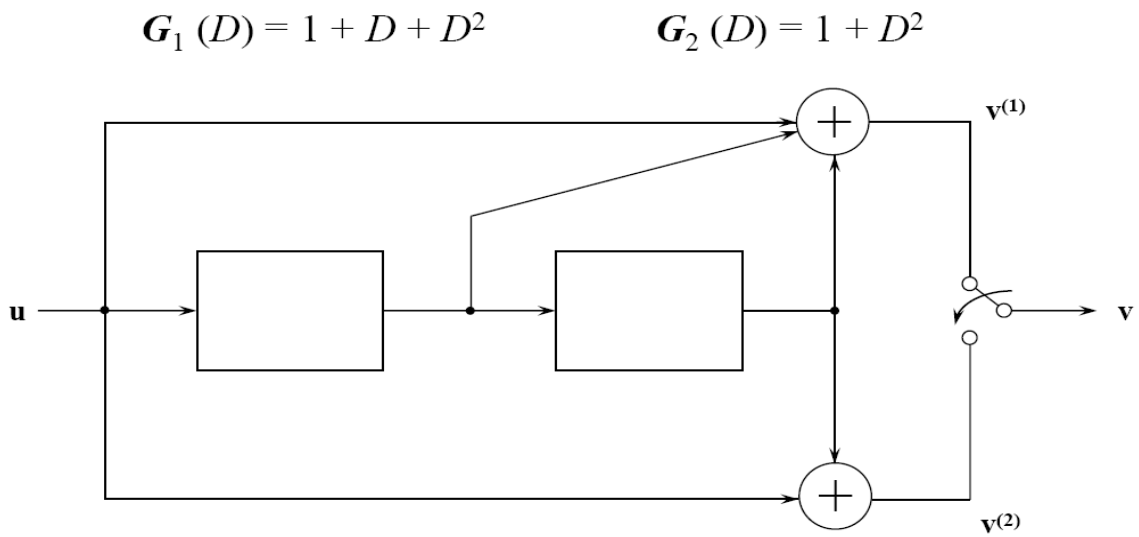

Figure 8. Code rate r=1/2, v=3 convolutional encoder. From [5]

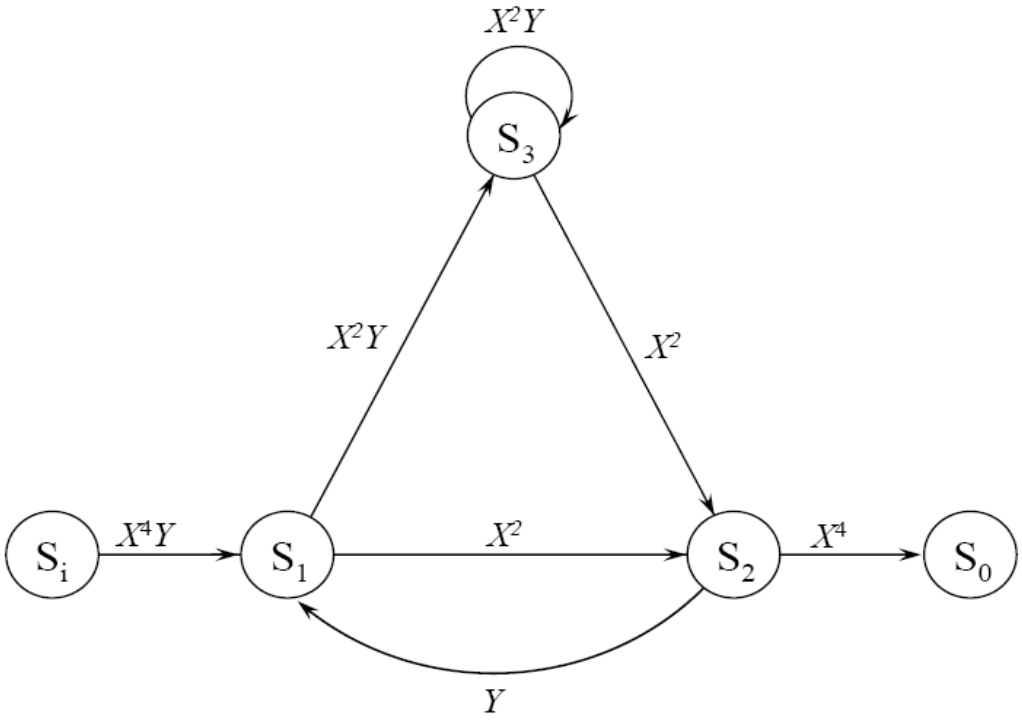

Figure 9. Signal flow graph for r=1/2, v=3 convolutional encoder with QPSK/TCM. From [5]

2. Probability of Bit Error

If TCM is implemented with 2^m–PSK or 2^m–QAM by using a convolutional encoder with code rate less than $r=m/m+1$, there will be parallel paths as shown in Figure 5. Generally speaking, parallel paths are unwanted because they limit the performance of a TCM system. This provides a lower bound beyond which the performance cannot be improved. The probability of sequence error is approximated by [5]

$$P_E \approx P_E(parallel) + A_{dfree_{nonparallel}} Q\left(\sqrt{\frac{E_{sc} d^2_{free_{nonparallel}}}{2N_0}}\right) \tag{2.3}$$

where $P_E(parallel)$ is the probability of not choosing the correct parallel path, $A_{dfree_{nonparallel}}$ is the average number of code sequences that are a distance $d_{free_{nonparallel}}$ from the correct code sequence, $d_{free_{nonparallel}}$ is the minimum squared-Euclidean distance between all possible sequences, and $E_{SC} = r(m+1)E_b$ [5]. For this thesis, where TCM is implemented with QPSK modulation and utilizing a $r=1/2$ convolutional encoder, $m=1$ *so* $E_{SC} = E_b$. The probability of bit error is approximated by [5]

$$P_b \approx P_b(parallel) + \frac{B_{dfree_{nonparallel}}}{m} Q\left(\sqrt{\frac{E_{sc} d^2_{free_{nonparallel}}}{2N_0}}\right) \tag{2.4}$$

where $P_b(parallel)$ is the probability of not choosing the correct parallel path and $B_{dfree_{nonparallel}}$ represents the information bit errors that are distance $d_{free_{nonparallel}}$ from the correct path [5].

In this chapter, basic TCM theory was reviewed. In the next chapter, the performance of a TCM system in AWGN is analyzed and compared with the other three non-TCM systems introduced in Chapter I.

THIS PAGE INTENTIONALLY LEFT BLANK

III. PERFORMANCE OF THE TCM SYSTEM AND THE ALTERNATIVES SYSTEMS IN AWGN

This chapter examines the performance in AWGN of four systems that occupy approximately the same bandwidth (for a fair comparison). AWGN unfortunately is always present even if no other noise sources are present. The performance of the TCM system with QPSK modulation is compared with the alternative system (QPSK modulation with code rate r=1/2 on the inphase and quadrature component). The comparison is also extended to two other systems, 8-BOK with code rate r=2/3 convolutional coding and 16-BOK with r=3/4 convolutional coding, since they almost have the same spectral efficiency as QPSK with convolutional coding.

A. INTRODUCTION

When forward error correction (FEC) is employed an upper bound on the probability of bit error is [6]

$$P_b < \frac{1}{k} \sum_{d=d_{free}}^{\infty} B_d P_d \tag{3.1}$$

where k is the number of information bits, d_{free} is the free distance of the convolutional code, B_d is the total number of information bit ones on all weight d paths, and P_d is the probability of selecting a code sequence a distance d from the correct code sequence. The total information weight B_d and the free distance depend on the convolutional code chosen, while P_d depends on the channel, the modulation scheme and the type of decoding used. In Table 1 are shown the best rate r=1/2 convolutional code weight structure.

Table 1. Best (maximum free distance) rate 1/2 convolutional code information weight structure. From [5]

v	d_{free}	B_{free}	B_{free+1}	B_{free+2}	B_{free+3}	B_{free+4}	B_{free+5}	B_{free+6}	B_{free+7}
3	5	1	4	12	32	80	192	448	1024
4	6	2	7	18	49	130	333	836	2069
5	7	4	12	20	72	225	500	1324	3680
6	8	2	36	32	62	332	701	2342	5503
7	10	36	0	211	0	1404	0	11633	0
8	10	2	22	60	148	340	1008	2642	6748
9	12	33	0	281	0	2179	0	15035	0

1. Probability of Bit Error (BER) with Hard Decision Decoding (HDD)

In HDD the receiver has two quantization levels in order to make "hard decisions" between binary one or zero. For HDD, the Hamming distance is the metric that is used. The probability P_d for hard decision decoding is [6]

$$\begin{aligned} P_d &= \sum_{i=\frac{d+1}{2}}^{d} \binom{d}{i} p^i (1-p)^{d-i} && \text{for } d \text{ odd} \\ P_d &= \frac{1}{2}\binom{d}{d/2} p^{d/2}(1-p)^{d/2} + P_d = \sum_{i=\frac{d+1}{2}}^{d} \binom{d}{i} p^i (1-p)^{d-i} && \text{for } d \text{ even} \end{aligned} \tag{3.2}$$

where p is the probability of channel bit error. Substituting P_d into Equation (3.1), we get the probability of bit error for hard decision decoding.

2. Probability of Bit Error (BER) with Soft Decision Decoding (SDD)

With SDD the receiver has more than two quantization levels and the demodulator makes "soft decisions". For TCM, the metric used is the squared Euclidean distance, as explained in Chapter II.

In obtaining the probability of bit error for SDD, Equation (3.1) is again used. The values for the coefficients B_d are listed in Table 2 for r=1/2 convolutional encoders. What is different now is the probability $P_{d.}$ In order to obtain P_d it is assumed that the receiver is a *maximal ratio combiner* (MRC). With the MRC, the conditional probability density function $\boldsymbol{f_r(r|v)}$ is maximized, where $\boldsymbol{v}$ is the correct code sequence and $\boldsymbol{r}$ is the received code sequence. The output of the demodulator is modeled as a Gaussian random variable with mean $\overline{r_k} = \sqrt{2}A_{C_k}$ and variance $\sigma_O{}^2 = N_O/T_{b_c}$ where $A^2{}_{C_k}$ is the average power of the received signal for the k^{th} channel bit, N_O is the one-sided noise power spectral density, and T_{b_c} is the duration of a coded bit $T_{b_c} = rT_b$ where T_b is the duration of a data bit. Assuming that the correct path is the all zero path and that the r^{th} path differs by d bits from the correct path, then a decoding error occurs when [2]

$$\sum_{k=1}^{d} r_k > 0 \tag{3.3}$$

where r_k is the output of the demodulator for the k^{th} channel bit. Now the probability P_d is [2]

$$P_d = P_r\left(\sum_{k=1}^{d} r_k > 0\right) \tag{3.4}$$

If X is the sum of d the independent random variables then [2]

$$X = \sum_{k=1}^{d} R_k \tag{3.5}$$

The mean of X is $\overline{X} = \sqrt{2}\sum_{k=1}^{d} A_{C_k}$ and the variance is $\sigma^2 = \sum_{k=1}^{d} \sigma_0^2$. Now P_d can be expressed with the Q-function as [2]

$$P_d = Q\left(\sqrt{\frac{\overline{X}^2}{\sigma^2}}\right) = Q\left(\sqrt{\frac{2dA_c^2}{\sigma_o^2}}\right) \tag{3.6}$$

where the variance $\sigma_o^2 = N_o/T_{b_c}$ represents the noise power due to AWGN and $A_{c_k} = A_c$ is assumed.

B. PERFORMANCE OF BPSK/QPSK

In Figure 10 the alternative system that is compared to TCM with QPSK modulation is shown. The data stream is separated on to the *inphase* and *quadrature* channels. Each channel with the r=1/2 convolutional encoder is equivalent to BPSK. The data rate is halved on the two channels. Supposing that there is one bit as input data, then there is *½ bit* on the inphase and *½ bit* on the quadrature channel. So there is a total of one bit per unit time. In reality it can be said that the odd bits are going in the inphase and the even bits in the quadrature channel, or the opposite. The total null-to-null bandwidth that this system occupies is $BW = 2R_S = R_{b_c} = 2R_b$, which is the bandwidth that BPSK without coding occupies.

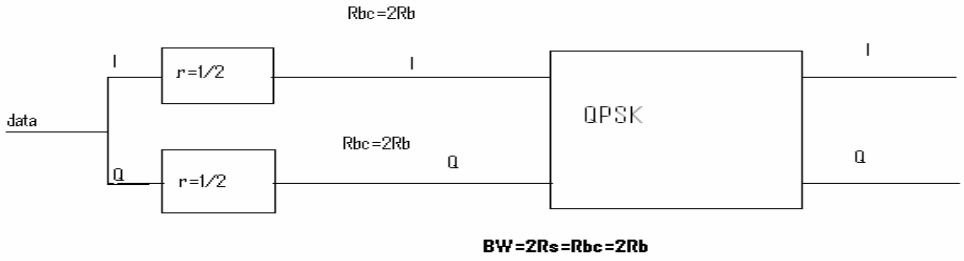

Figure 10. Overview of the alternative QPSK system

The bit error probability for BPSK/QPSK is [4]

$$P_b = Q\left(\sqrt{\frac{2E_b}{N_o}}\right) \tag{3.7}$$

where E_b/N_O is the signal-to-noise ratio, E_b is the average energy per bit and is given by $E_b = A_c^2 T_b$, where A_c^2 is the average received power of the signal, and T_b is the bit duration. If forward error correction (FEC) is used, then $E_{b_c} = rE_b$, where E_{b_c} is the

average energy per channel bit. In Equation (3.6), $\sigma_o^2 = N_o/T_{b_c}$ and $A_c^2 T_{b_c} = rE_b$ are substituted, yielding

$$P_d = Q\left(\sqrt{\frac{2drE_b}{N_o}}\right) \tag{3.8}$$

For QPSK modulation and convolutional encoding with code rate r=1/2, the probability of bit error for soft decision decoding is given by substituting (3.8) into (3.1), where generally only the first five non-zero terms are used:

$$P_b < \frac{1}{k}\sum_{d=d_{free}}^{d=d_{free}+4} B_d P_d \tag{3.9}$$

The first five terms are used since they dominate the summation. For r=1/2 codes, k=1 and the values of B_d are shown in Table 2 for several r=1/2 convolution encoders. Also in Table 2, the squared-Euclidean distances for different constraint lengths of the convolutional encoder are listed. In Figure 11 the performance of the alternative QPSK system for a variety of constraint lengths is shown.

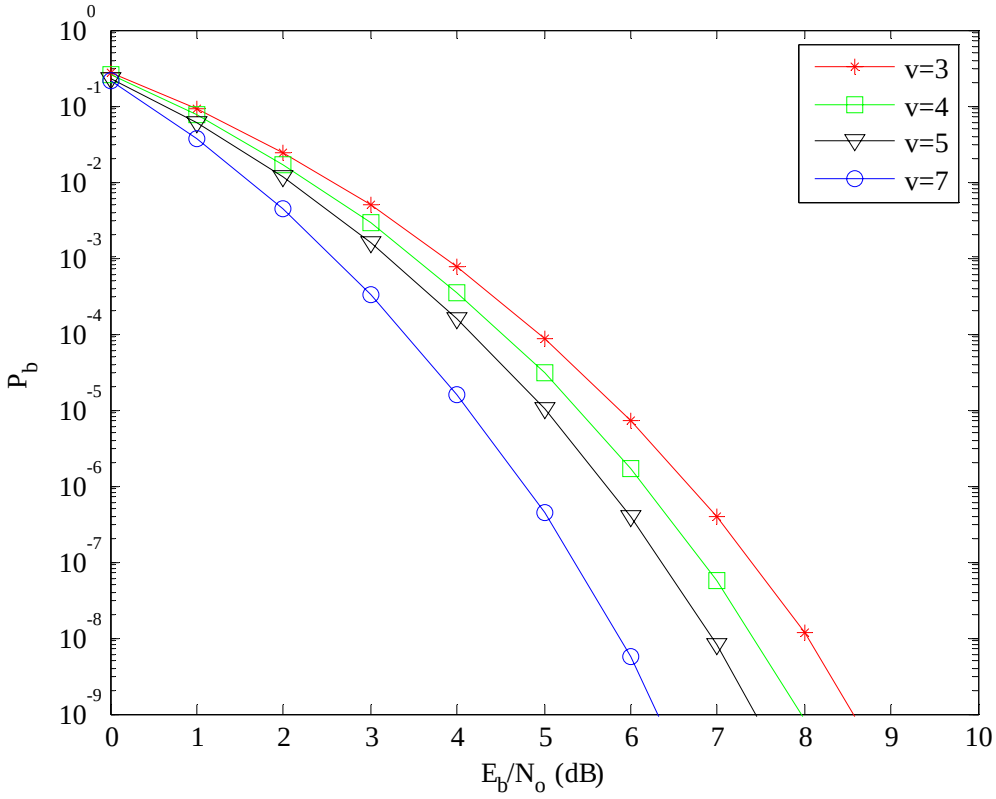

Figure 11. Performance of the alternative QPSK system with SDD, r=1/2 and various constraint lengths in AWGN

It is obvious that the performance improves as the constraint length increases. The corresponding SNR for obtaining $P_b=10^{-9}$ is *6.35* dB for constraint length seven and is *8.6* dB for constraint length three. For many practical applications, the required BER is $P_b=10^{-5}$. For this probability of bit error 4.141 dB are required for $v=7$ and *5.88* dB for v=3.

C. PERFORMANCE OF QPSK TCM IN AWGN

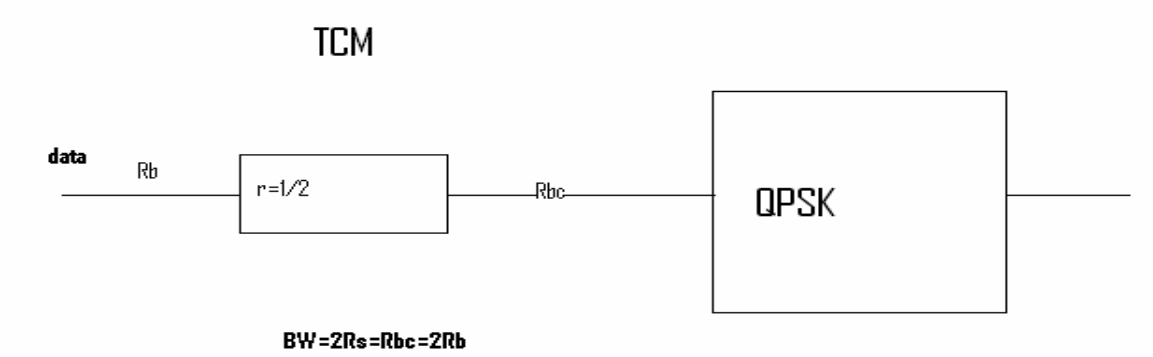

Figure 12. TCM with QPSK modulation and r=1/2 convolutional encoder

The approximate probability of bit error for a TCM system is given in Equation (2.4). The bandwidth for both systems (QPSK with r=1/2 and QPSK with TCM) is exactly the same. The null-to-null bandwidth for QPSK with TCM and r=1/2 convolutional encoding is $BW = 2R_s = 2R_{B_C}/2 = R_{B_C} = 2R_b$. For QPSK modulation with r=1/2 convolutional encoding there are no parallel paths. For a TCM system with no parallel transitions, like the one examined in this thesis, the probability of bit error is upper bounded by [5]

$$P_b < \frac{1}{m}\sum_{i=1}^{\infty} B_{d_i} Q\left(\sqrt{\frac{E_{s_c} d_i^2}{2N_0}}\right) \tag{3.10}$$

where B_{d_i} is the total number of the information bit errors for all paths that are a distance d_i^2 from the correct path. When i=1 then $d_1^2 = d_{free}^2$.

The values of the B_d coefficients are shown in Table 2. Careful scrutiny of Equations (3.9) and (3.10) reveals that for QPSK with r=1/2 convolutional encoding they are identical.

Table 2. Best (maximum squared-Euclidean distances) rate 1/2, convolutional code information weight structure. After [5]

v	d^2_{free}	B_{free}	B_{free+1}	B_{free+2}	B_{free+3}	B_{free+4}	B_{free+5}	B_{free+6}	B_{free+7}
3	10	1	4	12	32	80	192	448	1024
4	12	2	7	18	49	130	333	836	2069
5	14	4	12	20	72	225	500	1324	3680
6	16	2	36	32	62	332	701	2342	5503
7	20	36	0	211	0	1404	0	11633	0
8	20	2	22	60	148	340	1008	2642	6748
9	24	33	0	281	0	2179	0	15035	0

In Figure 13 the performance of the TCM system in AWGN is shown. As expected, performance improves as constraint length increases.

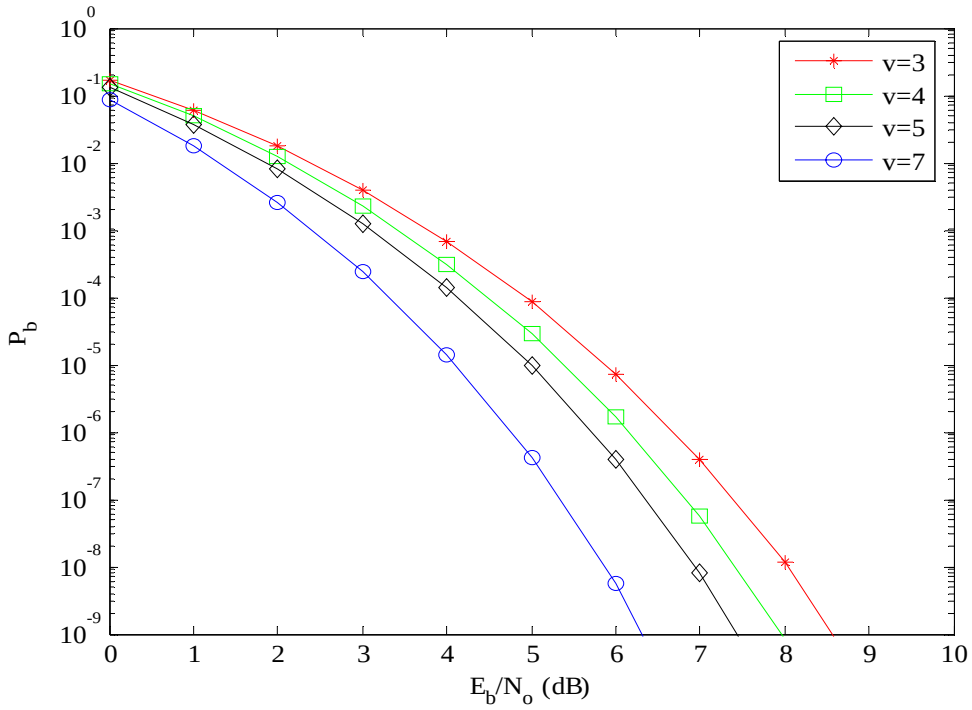

Figure 13. Performance of r=1/2 QPSK with TCM and various constraint lengths in AWGN

D. PERFORMANCE OF 8-BOK IN AWGN

One of the alternative systems that is compared to the TCM system is 8-BOK modulation with r=2/3 convolutional encoder. The null-to-null bandwidth for M-BOK is [7]

$$BW_{\min} = \frac{2^{q-1}+3}{2q} R_b \tag{3.11}$$

For 8-BOK, q=3, and the bandwidth expansion is 3/2 or *50%* because of the r=2/3 convolutional encoder. From Equation (3.10) the bandwidth for this system is

$$BW = \frac{7}{6} R_b \times \frac{3}{2} = \frac{21}{12} R_b \tag{3.12}$$

Hence, the bandwidth for 8-BOK is a little less than the two QPSK systems, so the comparison is not entirely fair. In contrast to the previous two systems, for the performance analysis of 8-BOK HDD is used instead of SDD. The reason is that after the demodulator a symbol-to-bit converter follows. Each symbol for 8-BOK consists of three bits and the difficulty is how to represent the 'soft decisions' at the bit level. The probability of symbol error for *M*-ary biorthogonal keying is [7]

$$P_s = 1 - \frac{1}{\sqrt{2\pi}} \int_{-\sqrt{2E_s/N_o}}^{\infty} e^{\left(\frac{-u^2}{2}\right)} \left[1 - 2Q\left(u + \sqrt{\frac{2E_s}{N_o}}\right)\right]^{\left(\frac{M}{2}-2\right)} du \tag{3.13}$$

The relationship between the probability of bit error and the probability of symbol error for *M*-BOK can be approximated by averaging the upper and the lower bound on bit error probability to obtain [7]

$$P_b \approx \left(\frac{1+q}{2q}\right) P_S = \left(\frac{1}{2q} + \frac{1}{2}\right) P_s \tag{3.14}$$

Also, the union bound for *M*-BOK is given [7]

$$P_s \le \left(2^q - 2\right) Q\left(\sqrt{\frac{E_s}{N_o}}\right) + Q\left(\sqrt{\frac{2E_s}{N_o}}\right) \tag{3.15}$$

Equations (3.13) and (3.15) have approximately the same simulation results.

Substituting Equation (3.13) or (3.15) into Equation (3.14), we obtain the probability making a channel bit error, and P_d is obtained from Equation (3.2). From Equation (3.1) the probability of bit error can be obtained. The B_{ds} for r=2/3 codes are listed in Table 3, where K is the number of memory elements in the convolutional encoder.

Table 3. Information weight structure for the best (maximum free distance) rate r=2/3 convolutional codes. After [5]

K	$\mathbf{d_{free}}$	$\mathbf{B_{dfree}}$	$\mathbf{B_{dfree+1}}$	$\mathbf{B_{dfree+2}}$	$\mathbf{B_{dfree+3}}$	$\mathbf{B_{dfree+4}}$
2	3	1	10	54	226	853
3	4	8	34	180	738	2989
4	5	25	112	357	1858	8406
5	6	75	0	1571	0	31474
6	6	1	81	402	1487	6793
7	8	395	0	6695	0	235288
8	8	97	0	2863	0	56633

In Figure 14 the performance of 8-BOK in AWGN with r=2/3 convolutional encoding and for a variety of constraint lengths is shown.

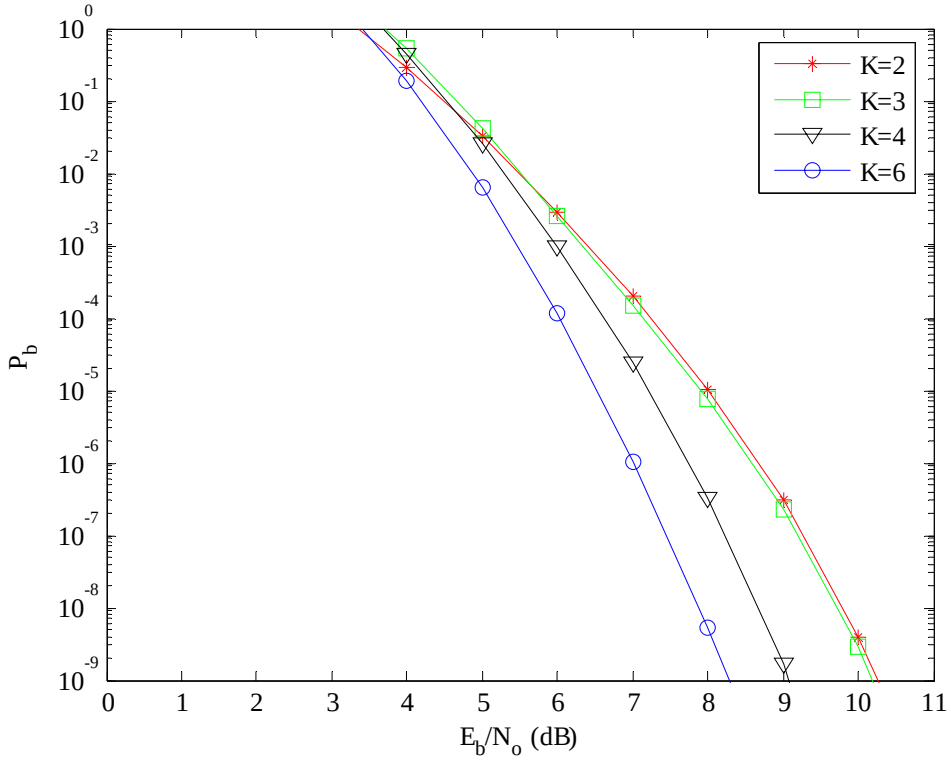

Figure 14. Performance of 8-BOK with r=2/3 convolutional encoding in AWGN for a variety of constraint lengths

Once again the performance improves as the number of memory elements increases. For $P_b=10^{-9}$ the corresponding SNR is *8.29* dB for *K=6*, almost 2 dB more compared with the *6.35* dB that QPSK TCM requires for constraint length seven. It is important to notice that constraint length seven is equivalent to *K=6*. In both cases the convolutional encoder has six memory elements. For $P_b=10^{-9}$ the required SNR is *10.28* dB for *K*=2, *1.69* dB more than the required SNR for QPSK TCM, which is *8.59* dB for constraint length three. For $P_b=10^{-5}$, *6.54* dB are required for *K=6*, 2.43 *dB* more than QPSK TCM and *8* dB for *K*=2, 2.12 dB more. It is obvious that in AWGN the performance of the 8-BOK r=2/3 is worse than the performance of the QPSK TCM system by about two dB and the difference increases as the number of memory elements increases.

E. PERFORMANCE OF 16-BOK IN AWGN

The last alternative system to be compared with QPSK TCM is 16-BOK modulation with r=3/4 convolutional encoder. The null-to-null bandwidth for M-BOK is obtained from Equation (3.10). For 16-BOK q=4, the bandwidth expansion is 4/3 *or* 33.3% because of the r=3/4 convolutional encoder. From Equation (3.10) the required bandwidth for this system is

$$BW = \frac{11}{8} R_b \times \frac{4}{3} = \frac{44}{24} R_b \tag{3.16}$$

The bandwidth for 16-BOK is again somewhat less than for the other two systems. By substituting Equation (3.13) or (3.15) into Equation (3.14), we obtain P_d from Equation (3.2). From Equation (3.1) the probability of bit error is obtained. The values for B_{ds} are obtained from Table 4, which is for code rate r=3/4 convolutional encoders.

Table 4. Information weight structure for the best (maximum free distance) rate r=3/4 convolutional codes. After [5]

K	d_{free}	B_{dfree}	$B_{dfree+1}$	$B_{dfree+2}$	$B_{dfree+3}$	$B_{dfree+4}$
2	3	15	104	540	2520	11048
3	4	124	0	4504	0	124337
4	4	22	0	1687	0	66964
5	5	78	572	3831	24790	152108
6	6	919	0	31137	0	1142571
6	5	21	252	1903	11995	72115
7	6	117	0	8365	0	319782
8	6	12	342	1996	12296	78145

In Figure 15 the performance of 16-BOK in AWGN with r=3/4 convolutional encoding and for a variety of constraint lengths is shown.

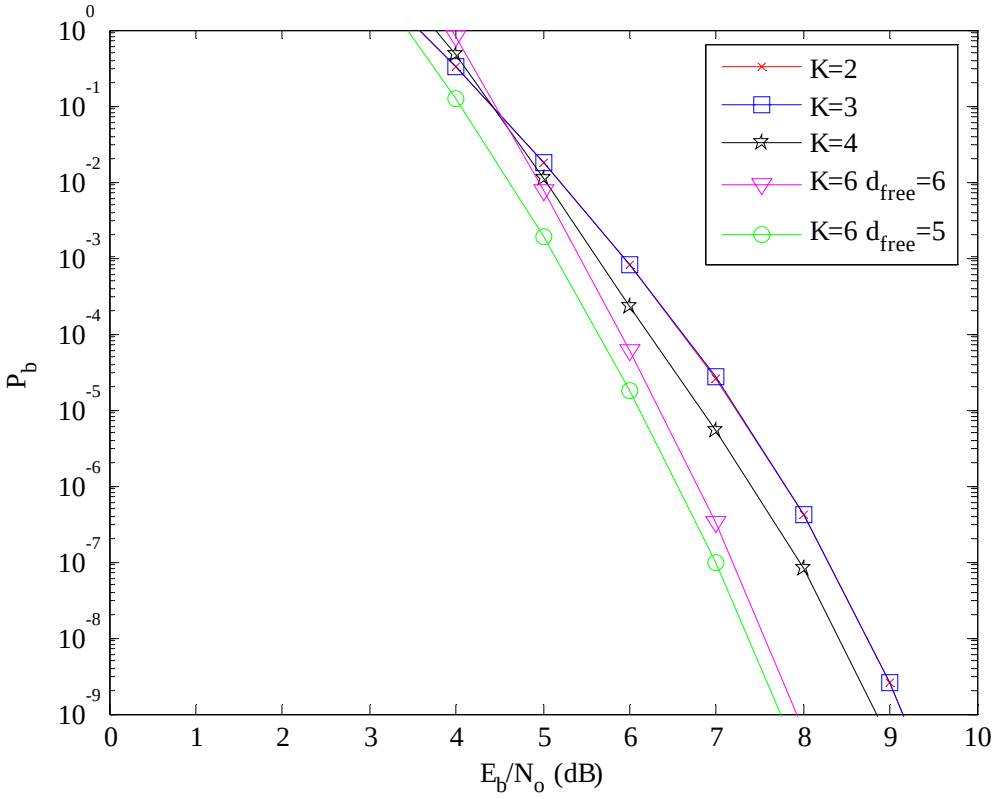

Figure 15. Performance of 16-BOK r=2/3 convolutional encoder for a variety of constraint lengths, in AWGN

Once again the performance improves as the number of memory elements increases. For $P_b=10^{-9}$ the corresponding SNR is *7.75* dB for $K=6$ with $d_{free=}5$ and *7.9*3 dB with $d_{free=}6$, almost 1.5dB more compared with the *6.*34 dB that QPSK TCM requires for constraint length seven. Noteworthy here is that for convolutional codes that are decoded using Viterbi algorithm, it is preferable to use codes with the largest free distances possible and having as the smallest possible total information weight $B_{dfree.}$ In Table 4 a careful look shows two codes with the same number of memory elements K=6. Although the first code has a larger free distance, its performance is slightly worse than the one with the smaller free distance. This is because the information weight of the second code is smaller. Although this is a secondary criterion, in this case B_{dfree} dominates the first criteria, which is the free distance. From now on in this thesis when there is a reference to 16-BOK with $K=6$, the second code with $d_{free=}5$ is meant. For $P_b=10^{-9}$, the required SNR is *9.16* dB for K=2, *0.57* dB more than the required SNR for

QPSK TCM, which is *8.59* dB for constraint length three. For $P_b=10^{-5}$ *6.*12 dB are required for *K=6*, 2 dB more than QPSK TCM, and *7.25* dB for *K*=2, 1.3*7* dB more. It is obvious that in AWGN, the performance of 16-BOK with *r*=3/4 encoding is better compared with the performance of 8-BOK with *r*=2/3 encoding and worse than the performance of QPSK TCM by about 1.*5* dB. The difference increases as the number of memory elements increases.

In this chapter, the performance in AWGN of the four systems under consideration has been analyzed. In the next chapters, the performance of those systems is analyzed in a pulse-noise interference environment.

THIS PAGE INTENTIONALLY LEFT BLANK

IV. PERFORMANCE OF THE TCM SYSTEM AND THE ALTERNATIVE QPSK SYSTEM IN AWGN PLUS PULSE-NOISE INTERFERENCE

A. PERFORMANCE ANALYSIS OF THE ALTERNATIVE QPSK SYSTEM

For SDD the probability of making a bit error by selecting a specific code sequence a distance *d* from the correct code sequence is given by Equation (3.6). In chapter three the performance was analyzed in AWGN. In this chapter, because of the pulse-noise interference, the noise power spectral density increases from N_o to $N_o + N_I$ where N_I is the power spectral density of the interferer. For a channel with pulse-noise interference

$$\sigma_k^2 = \begin{cases} \sigma_o^2 & \text{with probability 1-}\rho \\ \sigma_o^2 + \sigma_I^2 & \text{with probability } \rho \end{cases} \tag{4.1}$$

where $\sigma_o^2 = N_o / T_{b_c}$ is the noise power due to AWGN, $\sigma_I^2 = N_I / \rho T_{b_c}$ is the noise power due to pulse-noise interference, and ρ corresponds to the fraction of time that the pulse-noise interferer is on. The values of ρ are $0 < \rho \le 1$. For ρ=1 there is continuous or barrage noise interference. In Equation (3.6) only AWGN was assumed. If *d* independent bits are received and *i* of them are assumed to have interference, then the remaining *d-i* bits are affected only by AWGN. With pulse-noise interference, Equation (3.6) can be rewritten

$$P_d(i) = Q\left(\sqrt{\frac{\overline{X}^2}{\sigma^2}}\right) = Q\left(\sqrt{\frac{2d^2A_c^2}{d\sigma_o^2 + i\sigma_I^2}}\right) \tag{4.2}$$

Substituting the noise power due to AWGN $\sigma_o^2 = N_o / T_{b_c}$ and the noise power due to pulse-noise interference $\sigma_I^2 = N_I / \rho T_{b_c}$ into Equation (4.2), we get

$$P_d(i) = Q\left(\sqrt{\frac{2dA_c^2T_{b_c}}{N_0 + \frac{i}{d}\frac{N_I}{\rho}}}\right) = Q\left(\sqrt{\frac{2drE_b}{N_0 + \frac{i}{d}\frac{N_I}{\rho}}}\right) = Q\left(\sqrt{\frac{2dr}{\left(\frac{E_b}{N_0}\right)^{-1} + \frac{i}{d}\frac{1}{\rho}\left(\frac{E_b}{N_I}\right)^{-1}}}\right) \tag{4.3}$$

where $E_{b_c} = A_c^2 T_{b_c} = rE_b$. Now that $P_d(i)$, the conditional probability when i bits have interference and d-i bits are affected only by AWGN that a weight-d output sequence is selected, has been obtained, the average probability P_d of selecting a specific code sequence of weight d from the correct code sequence for all possible i is given by

$$P_d = \sum_{i=0}^{d} \binom{d}{i} \rho^i (1-\rho)^{d-i} P_d(i) \tag{4.4}$$

where ρ is the fraction of time that the interferer is operating. Recall that the probability of bit error is given by Equation (3.1), which is repeated here for convenience:

$$P_b < \frac{1}{k} \sum_{d=d_{free}}^{\infty} B_d P_d \tag{4.5}$$

In Equation (4.5) the values of the B_d for QPSK using r=1/2 error correction are obtained from Table 1, and P_d is given by Equation (4.4).

1. Performance of QPSK r=1/2 SDD Linear Combining for Constraint Length v=3 in a Pulse-Noise Interference Environment

With the values of B_d and d_{free} specified in Table 1 for constraint length v=3 and from Equations (4.4) and (4.5), the probability of bit error for QPSK with r=1/2 convolutional encoder and soft decision decoding (SDD) with linear combining (LC) is obtained. In Figure 16 the performance in a pulse-noise interference environment of a r=1/2, v=3 convolutional code with QPSK LC is shown.

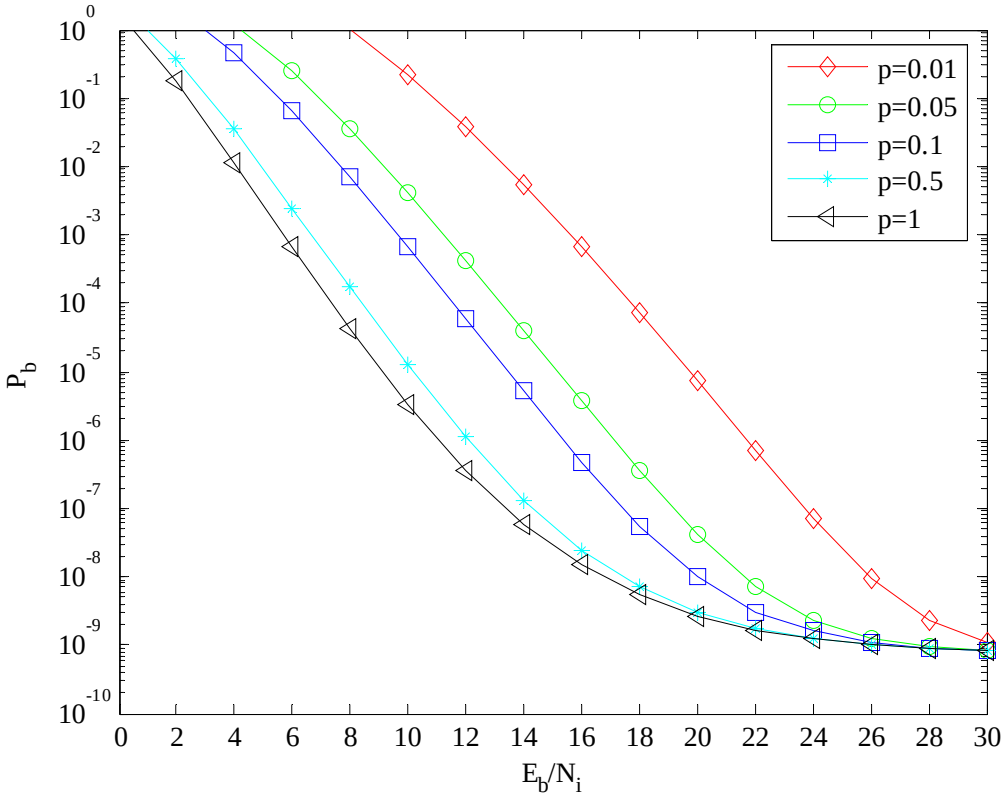

Figure 16. Performance of r=1/2, v=3 convolutional code with QPSK LC and PNI with E_b/N_o =8.673 dB

From Figure 16, it is obvious that pulse-noise interference is more effective than continuous (barrage) interference (ρ=1). Taking as a reference point the performance for P_b=10^{-5}, which is the BER used for many practical applications, 9.1dB of SIR required when interference is continuous (ρ=1), while for the same BER 19.7 dB is required when ρ=0.01. The comparison between the plots for ρ=1 and ρ=*0.0*1 yields a 10.6 dB difference for SNR=8.673 dB. In general the overall performance of the system shows no immunity at all to pulse-noise interference.

2. Performance of QPSK *r*=1/2 SDD Linear Combining for Constraint Length *v*=4 in a Pulse-Noise Interference Environment

With the values of B_d and d_{free} specified in Table 1 for constraint length v=4 and from Equations (4.4) and (4.5), the probability of bit error for QPSK with r=1/2

convolutional encoder and SDD with LC, is obtained. In Figure 17 the performance in a pulse-noise interference environment for a r=1/2, v=4 convolutional code with QPSK LC is shown.

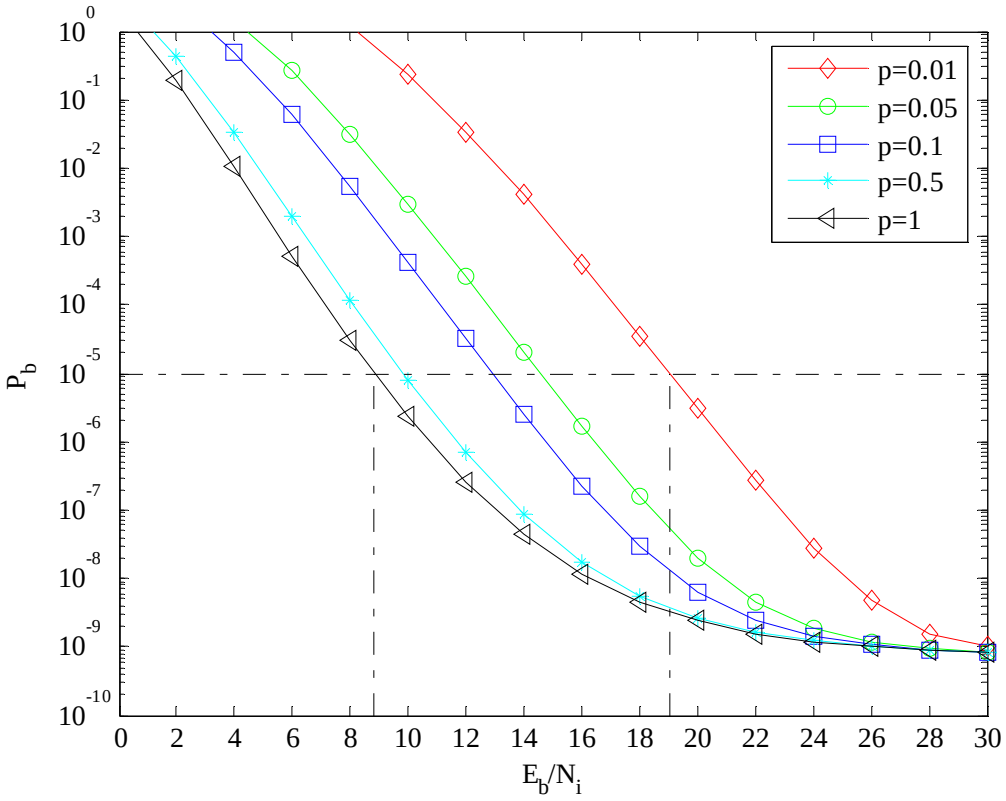

Figure 17. Performance of r=1/2, v=4 convolutional code with QPSK LC and PNI with E_b/N_o =8.040 dB

From Figure 17, it is apparent that the interfering signal is more efficient when employing pulse-noise interference. As ρ decreases the performance of the system worsens. Comparison between the curves for ρ=1 and ρ=0.01 yields 10.21dB difference for SNR=8.040dB. The required SNR for the same probability of bit error is less than in the last section due to the constraint length of the convolutional encoder, which has increased to v=4. Moreover, because of the increase in the constraint length, a small decrease in the difference between the curves for ρ=1 and ρ=0.01 of 0.41dB is observed, as compared with constraint length three. Nevertheless, the system continuous to show no immunity at all to pulse-noise interference.

3. Performance of QPSK *r*=1/2 SDD Linear Combining for Constraint Length *v=5* in a Pulse-Noise Interference Environment

The last constraint length considered is v=5. The values of B_d and d_{free} are specified in Table 1 for constraint length v=5. From Equations (4.4) and (4.5), the probability of bit error for QPSK with a r=1/2 convolutional encoder and SDD with LC, are obtained. In Figure 18 the performance in a pulse-noise interference environment for a r=1/2, v=4 convolutional code with QPSK LC is shown.

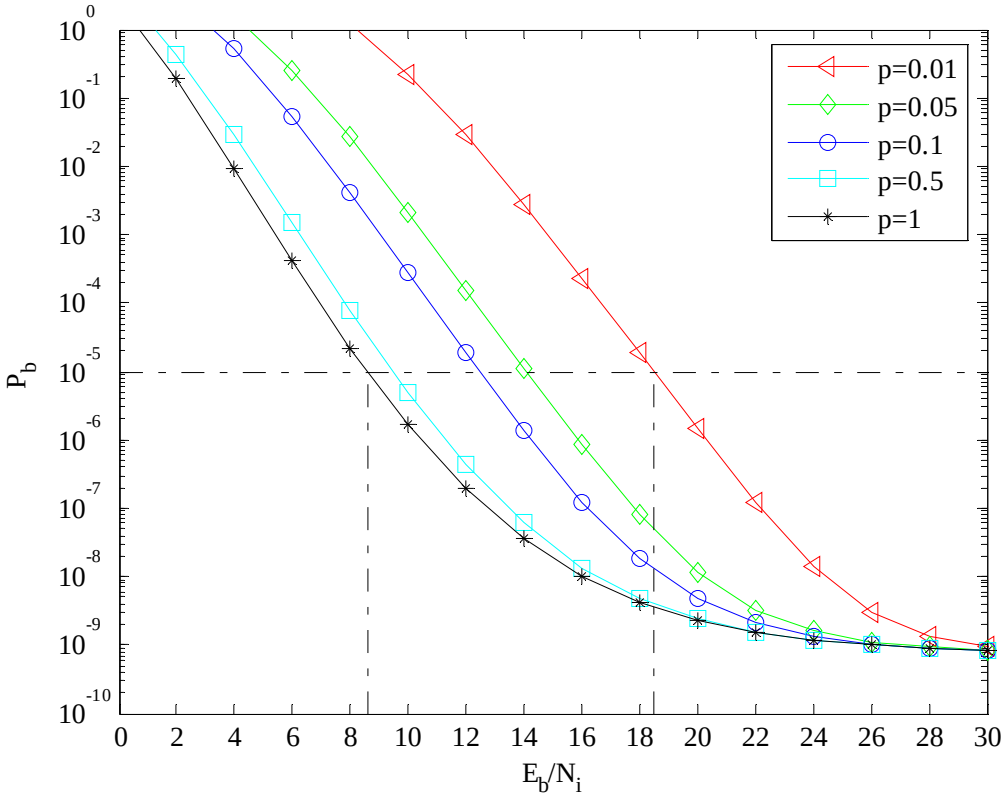

Figure 18. Performance of r=1/2, v=5 convolutional code with QPSK LC and PNI with E_b/N_o =7.523 dB

It is again obvious that as the fraction of time that the jammer is on decreases, the performance of the system worsens. The difference between the ρ=1 and ρ=0.01 plots has decreased to 9.9dB due to the increase in constraint length. Also, due to the increase in the constraint length, the required SNR is reduced to 7.523dB for the same probability

of bit error. As to the performance of the system, the same conclusion is reached. The system has no immunity to pulse-noise interference, and increasing the constraint length has very little effect.

B. PERFORMANCE ANALYSIS OF QPSK TCM SYSTEM

In chapter three the probability of bit error was evaluated only with AWGN. In a pulse-noise interference environment, the noise power due to pulse-noise interference is added to the existing noise power due to AWGN. For SDD the BER is obtained by substituting Equations (4.3) and (4.4) into Equation (4.5). For a TCM system in a pulse-noise interference environment, SDD is also used, but in order to calculate the probability of bit error, each path through the trellis must be treated independently. The modulation scheme used in this thesis is QPSK TCM with a r=1/2 convolutional encoder. This translates to no parallel paths as was explained in Chapter II. The performance of QPSK TCM using a r=1/2 convolutional encoder and a variety of constraint lengths is now analyzed.

1. Performance of *r*=1/2 Convolutional Code with QPSK TCM for Constraint Length *v*=3 in a Pulse-Noise Interference Environment

The convolutional encoder used for v=3 is shown in Figure 19. The trellis diagram for the TCM encoder with r=1/2, v=3 and no parallel paths/transitions, which corresponds to the encoder, is shown in Figure 20. In order to calculate the squared-Euclidean distances, Gray mapping is used as shown in Figure 7. From the trellis diagram, the minimum squared-Euclidean distance is found from the path $S_0 - S_1 - S_2 - S_0$ and is $d_{free}^2 = 10$. Only one path has this value of squared-Euclidean distance, and the information weight of this path is $B_{dfree} = 1$. Continuing, we find that the paths $S_0 - S_1 - S_2 - S_1 - S_2 - S_0$ and $S_0 - S_1 - S_3 - S_2 - S_0$ have squared-Euclidean distance $d_{free}^2 = 12$, and both have information weight $B_{dfree+1} = 4$.

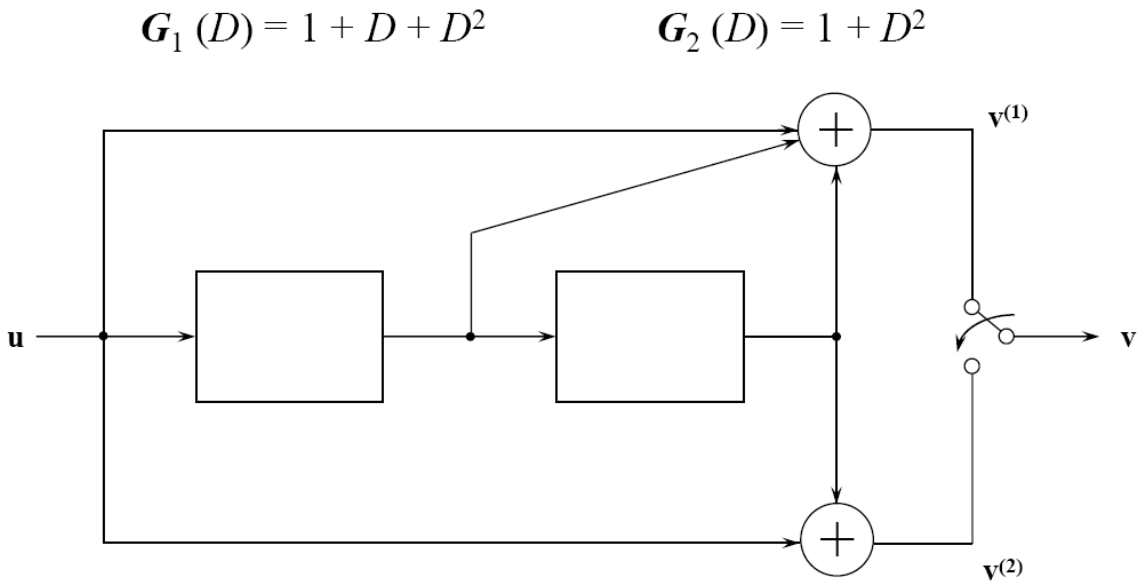

Figure 19. Rate r=1/2,v=3 convolutional code.From[5]

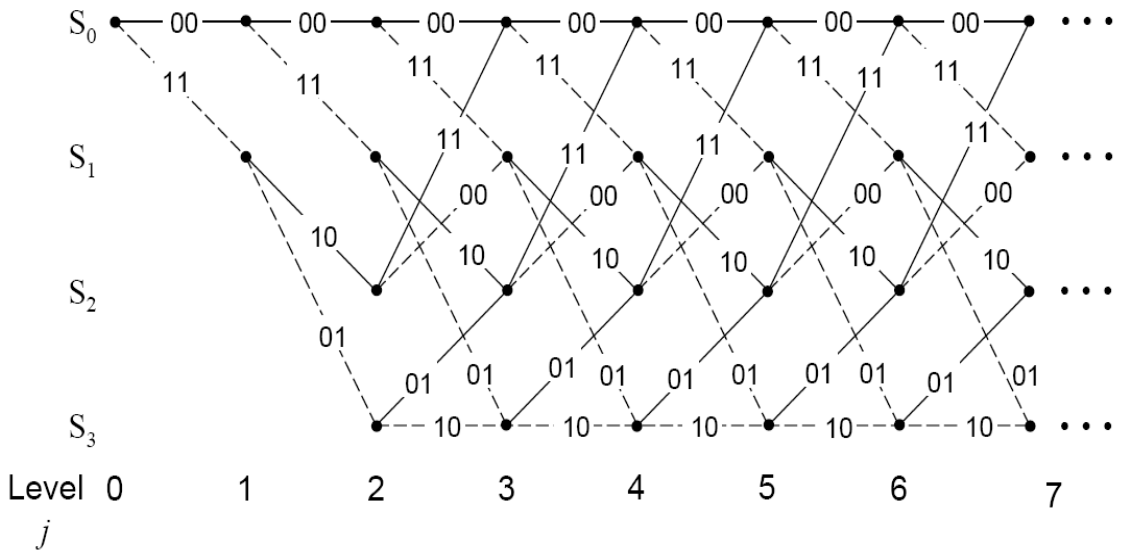

Figure 20. Trellis diagram for TCM encoder with r=1/2, v=3 and no parallel paths/transitions. From [5]

Accordingly, four paths are found with $d^2_{free} = 14$ and having total $B_{dfree+2} = 12$. All the values for r=1/2 convolutional codes and a variety of constraint lengths and

information weights are specified in Table 2. From Equation (3.10) the probability of bit error for a TCM system with no parallel transitions is repeated here for convenience:

$$P_b < \frac{1}{m}\sum_{i=1}^{\infty} B_{d_i} Q\left(\sqrt{\frac{E_{s_c} d_i^2}{2N_0}}\right) \tag{4.6}$$

where B_{d_i} is the total number of the information bit errors for all paths that are distance d_i^2 from the correct path. When i=1, then $d_1^2 = d_{free}^2$. In Chapter II it was noted that E_{sc} $=r(m+1)E_b$. In our case where TCM is implemented with QPSK modulation and utilizing a r=1/2 convolutional encoder, m=1 so E_{sc} $=E_b$. Since pulse-noise interference is now considered in addition to AWGN, we have $N_T = N_0 + N_I/\rho$, the total noise power spectral density due to AWGN plus the pulse-noise interference. The expression N_I/ρ denotes the interference power spectral density when the interferer is operating. Recall that ρ is the fraction of time that the interferer is on. The analytical evaluation of the probability of bit error P_b cannot be approximated by a general model, but must be calculated from each path in the trellis diagram independently. Let us take as an example the first path $S_0 - S_1 - S_2 - S_0$ with squared-Euclidean distance $d_{free}^2 = 10$. The number of the d received bits is three. We define i as the number of interfered bits. When i=0, none of the bits are affected by the pulse-noise interference. When i=1 one bit is affected by the pulse-noise interference and the other two only by AWGN. For this path, the maximum number of bits that can be affected is three. The probability of bit error for the r=1/2, v=3 convolutional code with QPSK TCM in a pulse-noise interference environment is approximated

$$P_b = B_{10}P_{10} + B_{12}P_{12} + B_{14}P_{14} + B_{16}P_{16} + B_{18}P_{18} + B_{20}P_{20} \tag{4.7}$$

where B_{10} is the information weight for the first path with $d_{free}^2 = 10$, B_{12} is the total information weight for the paths with $d_{free}^2 = 12$, and so on. It is generally accepted that the first four terms dominate the summation. P_{10} is the average probability of selecting a

specific code sequence of distance d^2 from the correct code sequence. Since i bits have interference and d-i bits do not, assuming that each bit is received independently, then for the first path where d=3

$$
\begin{aligned}
P_{10} &= (1-\rho)^3 Q\left(\sqrt{\frac{E_b}{N_0}\frac{10}{2}}\right) + && \text{when } i=0 \\
&+\rho(1-\rho)^2 Q\left\{\left(\sqrt{\frac{E_b}{2}\left(\frac{8}{N_0}+\frac{2}{N_T}\right)}\right)+2Q\left(\sqrt{\frac{E_b}{2}\left(\frac{6}{N_0}+\frac{4}{N_T}\right)}\right)\right\}+ && \text{when } i=1 \\
&+\rho^2(1-\rho)\ Q\left\{\left(\sqrt{\frac{E_b}{2}\left(\frac{2}{N_0}+\frac{8}{N_T}\right)}\right)+2Q\left(\sqrt{\frac{E_b}{2}\left(\frac{4}{N_0}+\frac{6}{N_T}\right)}\right)\right\}+ && \text{when } i=2 \\
&+\rho^3 Q\left(\sqrt{\frac{E_b}{N_T}\frac{10}{2}}\right) && \text{when } i=3
\end{aligned}
\tag{4.8}
$$

In the same manner P_{12} and the other $P_d s$ are calculated. All $P_d s$ used in this thesis are shown in the Appendix. Noteworthy is that for each P_d each path must be calculated independently if they are not of the same length. For example, for P_{12} two paths exist with $d_{free}^2 = 12$ but with different lengths. So from Figure 20 it can be seen that if interference occurs at time index 2 to 3, one path will be affected but the other will not because it is a zero path and moreover does not carry an information bit. As a consequence, the P_d for the two paths cannot be calculated in the same way. From Equation (4.8) and Table 2 where the values of the B_d coefficients are specified, the probability of bit error for QPSK TCM using a r=1/2 convolutional encoder with constraint length v=3 is obtained. The performance of the system for a variety of values of ρ is shown in Figure 21.

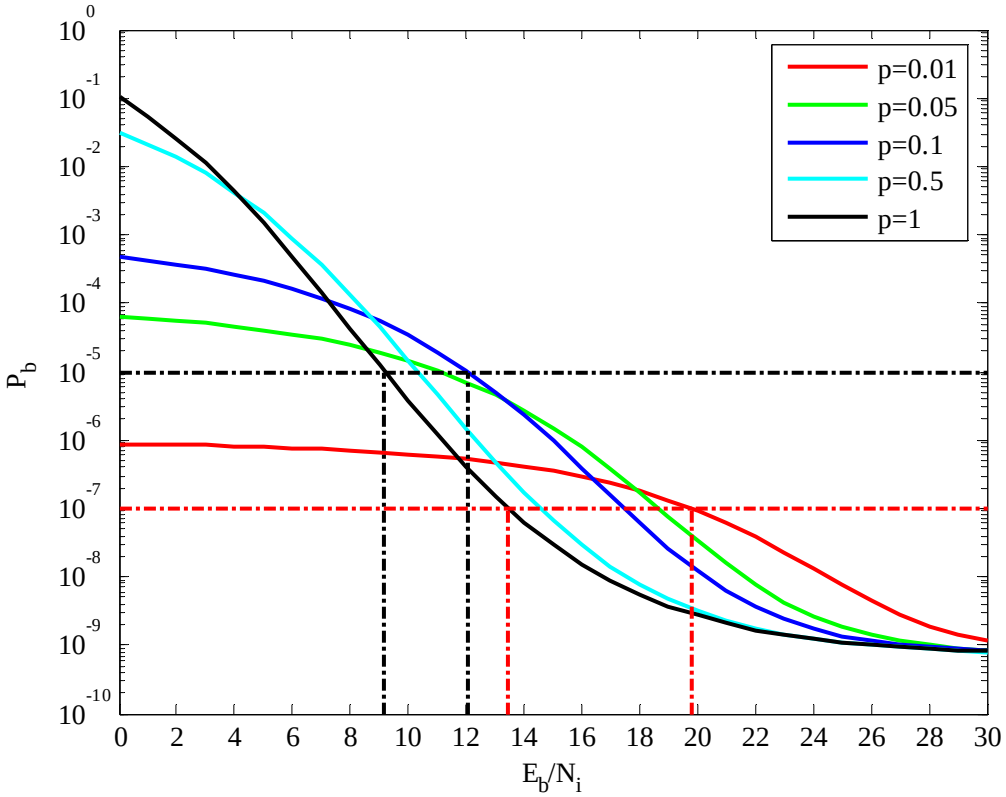

Figure 21. Performance of r=1/2,v=3 convolutional code with QPSK TCM PNI and E_b/N_o =8.691 dB

It is obvious that as ρ decreases the performance of the system is dependent on E_b/N_I and P_b. For P_b=10^{-5}, there is a slight degradation of 2.858dB due to pulse-noise interference, while at BER P_b=10^{-7} the degradation increases to 5.212 dB.

2. Performance of r=1/2 Convolutional Code with QPSK TCM for Constraint Length v=4 in a Pulse-Noise Interference Environment

In Figure 22 and in Figure 23 the encoder and the trellis diagram for the TCM encoder with r=1/2, v=4 and no parallel paths/transitions are shown, respectively. The dotted lines in the diagram represent a decoded bit one, while the black lines represent a decoded bit zero. From the trellis diagram, the minimum squared-Euclidean distance is found from the path $S_0 - S_1 - S_3 - S_6 - S_4 - S_0$ and is $d_{free}^2 = 12$. Only one path has this

$$\boldsymbol{G}_1(D) = 1 + D^2 + D^3 \qquad \boldsymbol{g}^{(1)} = (1\ 0\ 1\ 1)$$

$$\boldsymbol{G}_2(D) = 1 + D + D^2 + D^3 \qquad \boldsymbol{g}^{(2)} = (1\ 1\ 1\ 1)$$

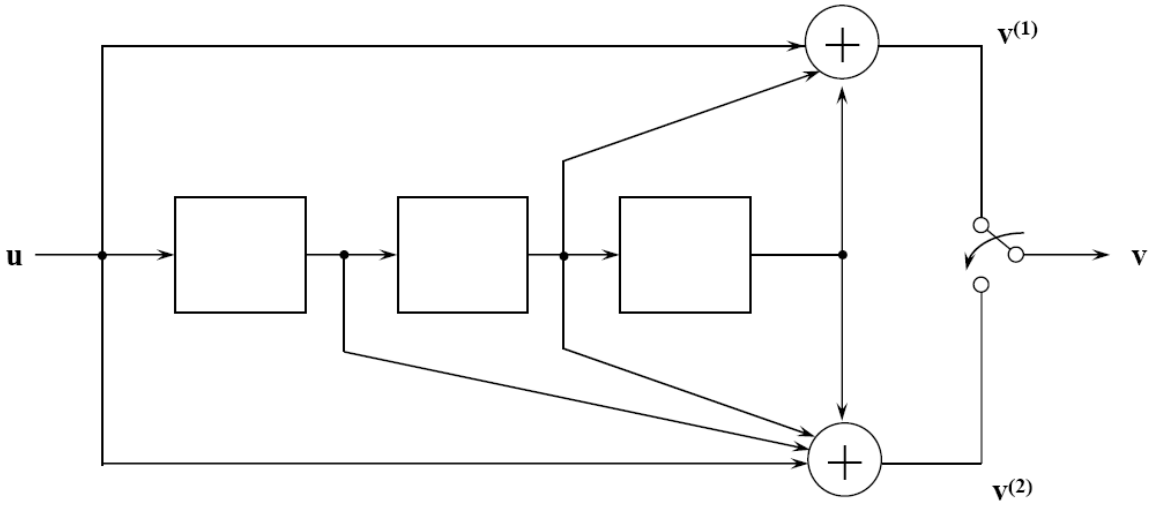

Figure 22. Rate r=1/2, v=4 convolutional code. From[5]

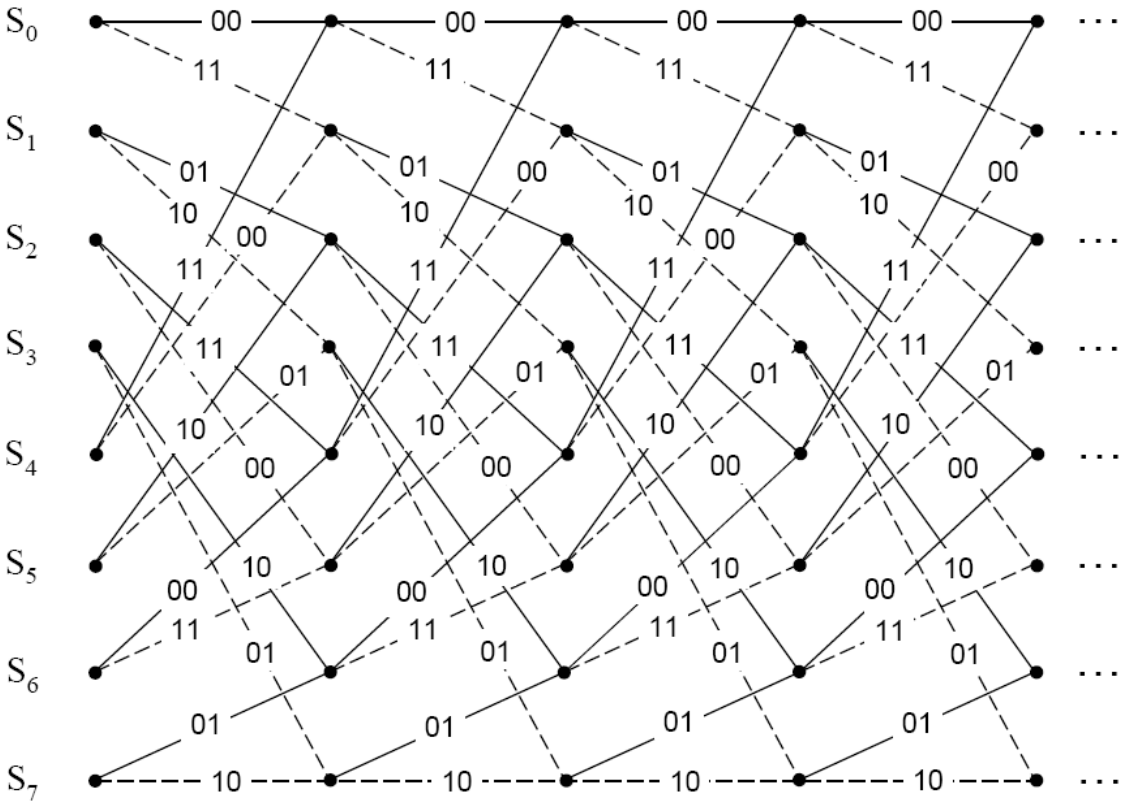

Figure 23. Trellis diagram for TCM encoder with r=1/2, v=4 and no parallel paths/transitions. From [5]

value of squared-Euclidean distance, and the information weight of this path is $B_{dfree} = 2$. Continuing the procedure, we find that the paths $S_0 - S_1 - S_2 - S_5 - S_3 - S_6 - S_4 - S_0$ with $B_{dfree+1} = 3$, $S_0 - S_1 - S_2 - S_4 - S_0$ with $B_{dfree+1} = 1$ and $S_0 - S_1 - S_3 - S_7 - S_6 - S_4 - S_0$ with $B_{dfree+1} = 3$ have squared-Euclidean distance $d^2_{free} = 14$, and the three of them have a total information weight $B_{dfree+1} = 7$, as specified in Table 2 for r=1/2 and constraint length v=4. The probability of bit error for the r=1/2, v=4 convolutional code with QPSK TCM in a pulse-noise interference environment is approximated

$$P_b = B_{12}P_{12} + B_{14}P_{14} + B_{16}P_{16} + B_{18}P_{18} + B_{20}P_{20} + B_{22}P_{22} \tag{4.9}$$

where B_{12} is the information weight for the first path with $d^2_{free} = 12$, B_{14} is the total information weight for the paths with $d^2_{free} = 14$, and so on. From Equation (4.9) and Table 2, where the B_d coefficients are specified, the probability of bit error for QPSK TCM using a r=1/2 convolutional encoder and constraint length v=4 is obtained. The performance of the system for a variety values of ρ is shown in Figure 24.

Once again is obvious that as ρ decreases the performance of the system gets worse and then better. Taking as a reference point, we see that for a probability of bit error of P_b=10^{-5} a slight degradation of 1.685 dB due to pulse-noise interference is observed. At BER P_b=10^{-7} the degradation increases to 3.9 dB. It is noteworthy that the required SNR for the same P_b is less as compared with constraint length v=3. Moreover, the system shows better immunity to pulse-noise interference. At P_b=10^{-5} the degradation is 1.17 dB less, while at P_b=10^{-7} it is 1.31 dB less, as compared with v=3.

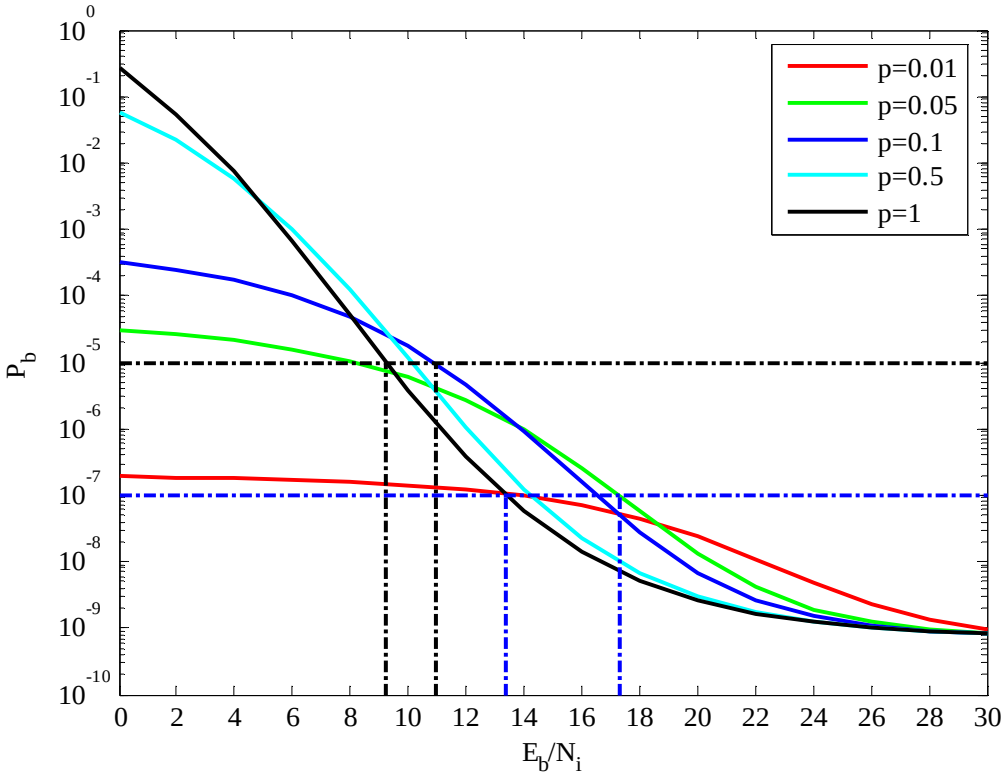

Figure 24. Performance of r=1/2,v=4 convolutional code with QPSK TCM PNI and E_b/N_o =8.123 dB

3. Performance of *r*=1/2 Convolutional Code with QPSK TCM for Constraint Length *v=5* in a Pulse-Noise Interference Environment

The probability of bit error for the r=1/2, v=5 convolutional code with QPSK TCM in a pulse-noise interference environment is approximated

$$P_b = B_{14}P_{14} + B_{16}P_{16} + B_{18}P_{18} + B_{20}P_{20} + B_{22}P_{22} + B_{24}P_{24} \tag{4.10}$$

where $B_{14} = 4$ is the information weight for the first two paths with $d_{free}^2 = 14$, $B_{16} = 12$ is the total information weight for the paths with $d_{free}^2 = 16$, and so on. From Equation (4.10) and Table 2 where the values of the B_d coefficients are specified, the probability of bit error for QPSK TCM using r=1/2 convolutional encoder and constraint length v=5 can be obtained. The performance of the system for a variety of values of ρ is shown in Figure 25.

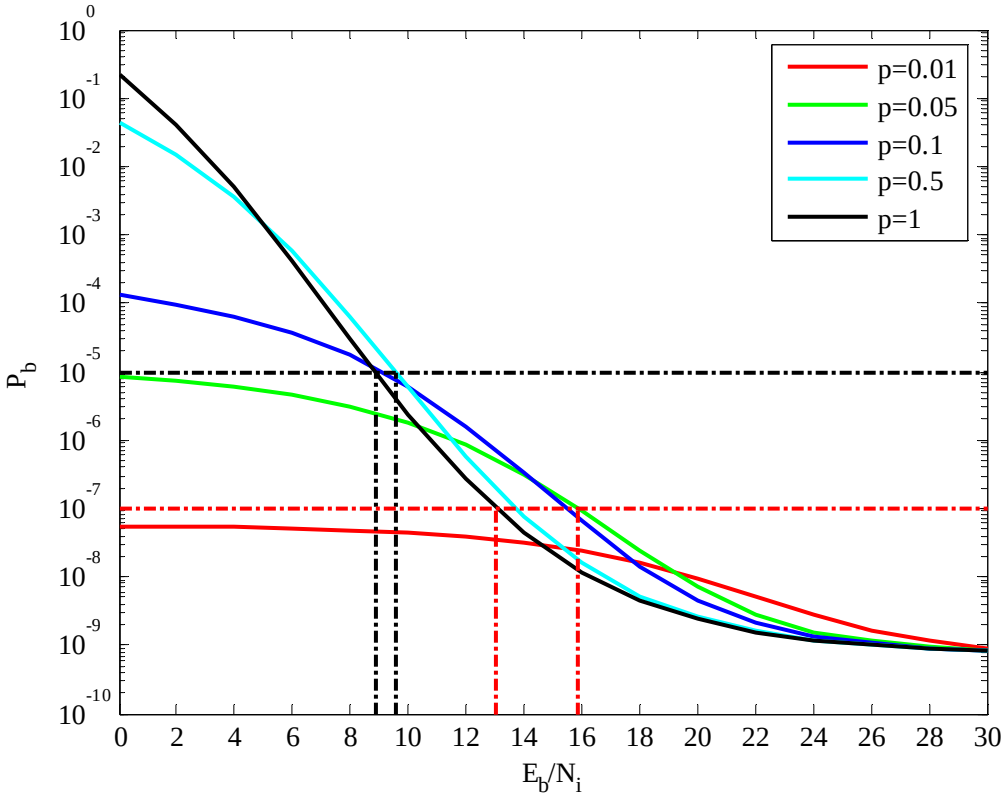

Figure 25. Performance of r=1/2,v=5 convolutional code with QPSK TCM PNI and E_b/N_o =7.68 dB

Once again is obvious that as ρ decreases the performance of the system first worsens and then improves. Taking as a reference point $P_b=10^{-5}$, we observe a very slight degradation of 0.69 dB due to pulse-noise interference, almost 1 dB less than for constraint length v=4 and 2.16 dB less than for constraint length v=3. At $P_b=10^{-7}$ the degradation of the system increases to 2.82 dB but is still almost 1 dB less than for constraint length v=4 and 2.39 dB less than for constraint length v=3. It is also noteworthy that the required SNR for the same P_d is less as compared with constraint length v=4 and v=3. It is obvious that the system shows larger immunity to pulse-noise interference as compared with v=3 and v=4. Summarizing, we see that as the constraint length increases, the performance of the TCM system improves and presents more resistance to pulse-noise interference.

C. COMPARISON OF THE TWO SYSTEMS IN A PULSE-NOISE INTERFERENCE ENVIRONMENT

So far two systems which occupy exactly the same bandwidth $2R_b$ have been analyzed. To compare the performance obtained from both, QPSK modulation with r=1/2 convolutional code with SDD LC and QPSK modulation with TCM, r=1/2 with SDD, the performance of the two systems is plotted together for various values of ρ but with the same value of constraint length.

1. Comparison of r=1/2 QPSK TCM with r=1/2 QPSK SDD LC both with Constraint Length v=3

In Figure 26 the performance of the two systems is shown for constraint length v=3.

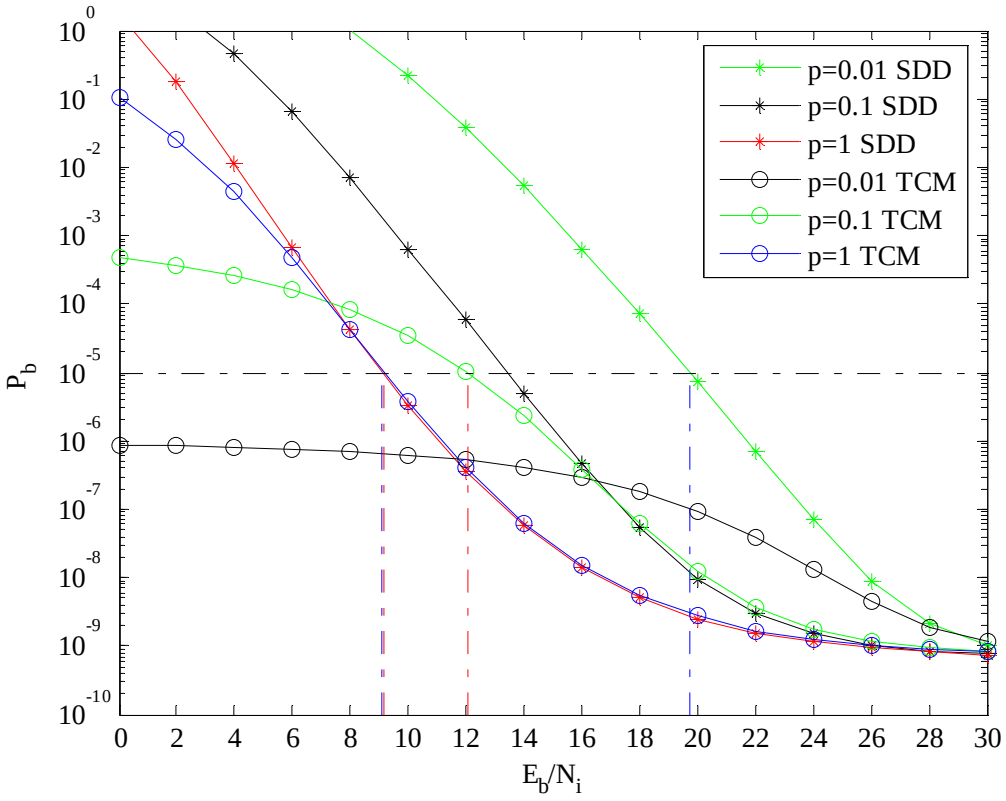

Figure 26. Comparison of r=1/2,v=3 convolutional code with QPSK TCM PNI and r=1/2, v=3 convolutional code with QPSK LC and PNI with E_b/N_o =8.691 dB

The SNR is 8.691 dB, and is the required SNR for the TCM system to obtain $P_b = 10^{-9}$ in a continuous interference environment when the SIR is 26 dB. From Figure 26, taking as a reference the performance for $P_b = 10^{-5}$, the comparison between the curves for ρ=1 and ρ=*0.*1 for the TCM system yields a difference of 2.858 dB, which can be translated as a degradation of the system due to pulse-noise interference. In contrast, the difference between the curves for the QPSK LC system for ρ=1 and ρ=*0.0*1 at $P_b = 10^{-5}$ yields a difference of 10.6 dB, nearly 8 dB more than the TCM system. The TCM system in general has better performance for smaller values of ρ. On the other hand, the QPSK LC system performance worsens for smaller values of ρ. Finally, it is obvious that even for constraint length v=3 the TCM system shows great immunity to pulse-noise interference while the QPSK SDD LC shows no immunity at all.

2. Comparison of *r*=1/2 QPSK TCM with *r*=1/2 QPSK SDD LC both with Constraint Length *v*=4

The performance of the two systems for constraint length v=4 is shown in Figure 27. The required SNR for the TCM system to obtain $P_b = 10^{-9}$ in a continuous interference environment is SNR=8.123 dB, which is less than for constraint length v=3. From Figure 27 taking as a reference the performance for $P_b = 10^{-5}$, the comparison between the curves for ρ=1 and ρ=*0.*1 for the TCM system yields a difference of 1.685 dB, which can be translated as a degradation of the system due to pulse-noise interference. In contrast the difference between the curves for QPSK LC system for ρ=1 and ρ=*0.0*1 at $P_b = 10^{-5}$ yields a difference of 10.21 dB. It is obvious that for constraint length v= 4 the TCM system shows greater immunity to pulse-noise interference than for constraint length v=3. Again, QPSK with SDD LC with v=4 shows no immunity at all.

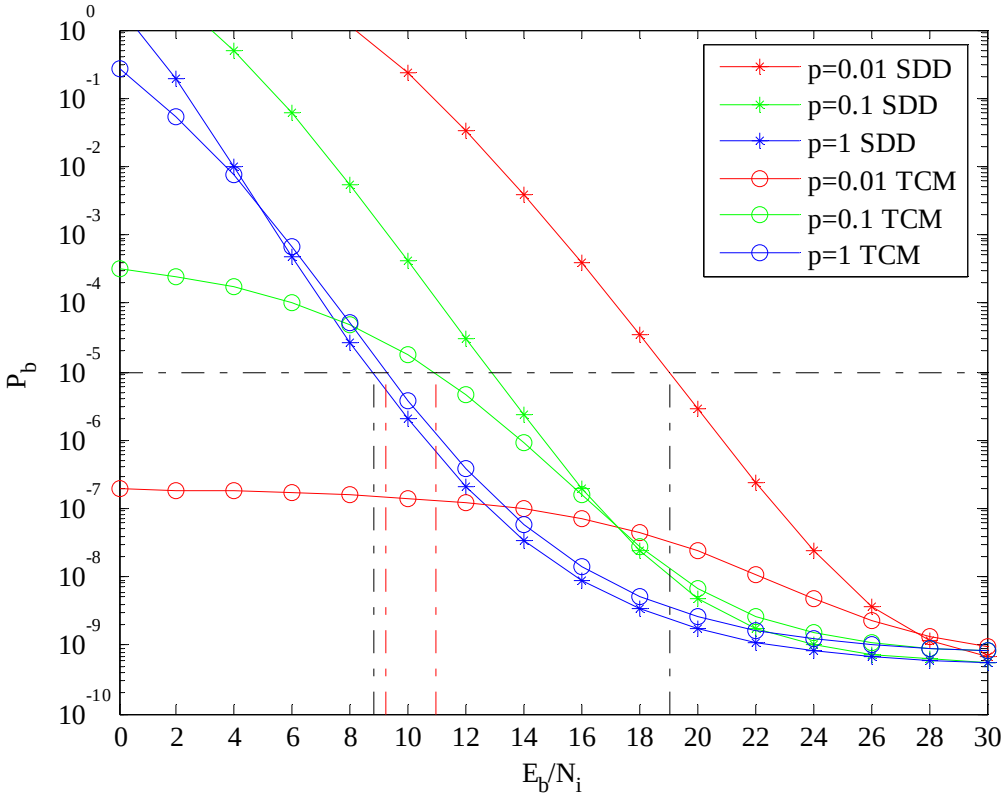

Figure 27. Comparison of r=1/2,v=4 convolutional code with QPSK TCM PNI and r=1/2, v=4 convolutional code with QPSK LC and PNI with E_b/N_o =8.123 dB

3. Comparison of *r*=1/2 QPSK TCM with *r*=1/2 QPSK SDD LC both with Constraint Length *v=5*

Finally, in Figure 28 both systems are plotted for constraint length v=5. Because of the increase of the constraint length the required SNR for the same BER is reduced to 7.68dB. At $P_b = 10^{-5}$, the degradation of the TCM system is reduced to 0.69 dB due to pulse-noise interference. In contrast the difference between the curves for QPSK LC system for ρ=1 and ρ=*0.0*1 at $P_b = 10^{-5}$ yields a difference of 9.9 dB, more than 9 dB more than the TCM system. It is obvious that for constraint length v= *5* that the TCM system shows greater immunity to pulse-noise interference than for constraint lengths v=3 and v=4. On the contrary, QPSK with SDD LC with v=*5* once again shows no immunity at all.

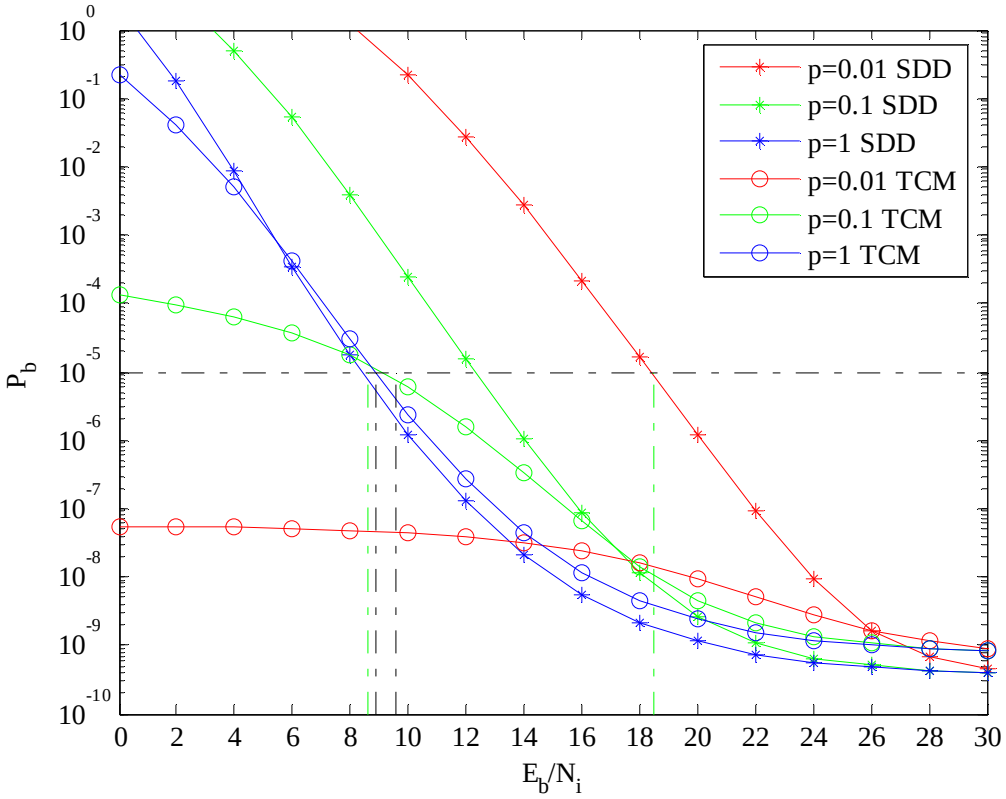

Figure 28. Comparison of r=1/2,v=5 convolutional code with QPSK TCM PNI and r=1/2, v=5 convolutional code with QPSK LC and PNI with E_b/N_o =7.68 dB

In this chapter the performance of two systems, QPSK TCM with a r=1/2 convolutional encoder and QPSK LC with a r=1/2 convolutional code, both with SDD decoding and in a pulse-noise interference environment, were examined. In the next chapter the analysis of two additional alternative systems which occupy approximately the same bandwidth as the TCM system is continued for a pulse-noise interference environment.

V. PERFORMANCE OF 8-BOK AND 16-BOK IN AWGN PLUS PULSE-NOISE INTERFERENCE

In this chapter the performance of 8-BOK with code rate r=2/3 and 16-BOK with code rate r=3/4 in a pulse-noise interference environment is examined for a variety of constraint lengths. The occupied bandwidth of both systems is approximately the same compared with the bandwidth that the TCM system occupies, as was mentioned in Chapter III. Also the performance of the TCM system is compared with the systems examined in this chapter.

A. PERFORMANCE ANALYSIS OF 8-BOK WITH *R*=2/3 CONVOLUTIONAL ENCODER, IN PULSE-NOISE INTERFERENCE ENVIRONMENT

One of the alternative systems which is compared to the TCM system is 8-BOK modulation with r=2/3 convolutional encoder. The null-to-null bandwidth for M-BOK is given from Equation (3.11), and for the 8-BOK is $BW = 21/12\,R_b$ as mentioned in Equation (3.12). The bandwidth for 8-BOK is a little bit less than the other two systems, as has already been mentioned. The occupied bandwidth for the two systems in Chapter IV is $BW = 2R_b$. In contrast with the previous two systems, for the performance analysis of 8-BOK, hard decision decoding (HDD) is assumed. The reason, as was mentioned in Chapter III, is the difficulty in the representation of the 'soft decisions' at the bit level because each symbol for 8-BOK represents three bits. The probability of symbol error for M-ary biorthogonal keying when only AWGN is present is approximated in Equation (3.13). In this chapter, because of the pulse-noise interference, the noise power spectral density increases from N_o to $N_o + N_I$ where N_I is the power spectral density of the interferer. Accordingly, the probability of symbol error for M-ary biorthogonal keying when pulse-noise interference is present in addition to AWGN can be approximated.

$$P_s = 1 - \frac{1}{\sqrt{2\pi}} \int_{-\sqrt{\frac{2E_s}{N_o + \frac{N_I}{\rho}}}}^{\infty} e^{\left(\frac{-u^2}{2}\right)} \left[1 - 2Q\left(u + \sqrt{\frac{2E_s}{N_o + \frac{N_I}{\rho}}} \right) \right]^{\left(\frac{M}{2}-2\right)} du \qquad (4.11)$$

The expression N_I/ρ denotes that the interference power spectral density when the interferer is operating. The relationship between the probability of bit error and the probability of symbol error for M-BOK in AWGN is approximated in Equation (3.14) and repeated here

$$P_b \approx \left(\frac{1+k}{2k}\right)P_s = \left(\frac{1}{2k}+\frac{1}{2}\right)P_s \tag{4.12}$$

Also, the union bound for M-BOK is approximated from Equation (3.15) only for AWGN. In pulse-noise interference environment, the union bound can be approximated

$$P_s \le \left(2^q-2\right)Q\left(\sqrt{\frac{rqE_b}{N_o+\frac{\mathrm{N_I}}{\rho}}}\right)+Q\left(\sqrt{\frac{2rqE_b}{N_o+\frac{\mathrm{N_I}}{\rho}}}\right) \tag{4.13}$$

where q=3 for 8-BOK and the convolution encoder used in order to meet the bandwidth requirements is r=2/3. Equations (5.1) and (5.3) have approximately the same numerical results in a pulse-noise interference environment. By substituting Equation (5.1) or (5.3) into Equation (5.2), we get $P_b(N_I)$, which is the probability of bit error in a pulse-noise interference environment when the interferer is operating. The average probability of bit error is given by

$$p = \rho P_b\left(N_I\right)+(1-\rho)P_b(N_0) \tag{4.14}$$

where ρ is the fraction of time the interferer is on and $P_b(N_0)$ is the probability of bit error in AWGN. The probability of selecting a specific code sequence a distance d from the correct code sequence P_d is obtained for HDD from Equation (3.2), which is repeated here for convenience:

$$P_d = \begin{cases} \displaystyle\sum_{i=\frac{d+1}{2}}^{d}\binom{d}{i}p^i(1-p)^{d-i} & \text{for } d \text{ odd} \\ \displaystyle\frac{1}{2}\binom{d}{d/2}p^{d/2}(1-p)^{d/2}+P_d = \sum_{i=\frac{d+1}{2}}^{d}\binom{d}{i}p^i(1-p)^{d-i} & \text{for } d \text{ even} \end{cases} \tag{4.15}$$

where p is the probability of the channel bit error and is given by Equation (5.4). As previously discussed in Chapter III and for convenience repeated here, the upper bound on the probability of bit error with forward error correction with FEC is

$$P_b < \frac{1}{k} \sum_{d=d_{free}}^{\infty} B_d P_d \tag{4.16}$$

From Equation (5.6) the probability of bit error can be obtained. P_d is known from Equation (5.5) and the B_d coefficients are specified in Table 3.

1. Performance of 8-BOK with r=2/3 and K=2 Convolutional Code in a Pulse-Noise Interference Environment

In Figure 29 the performance of 8-BOK with a r=2/3, K=2 convolutional encoder in a pulse-noise interference environment is shown.

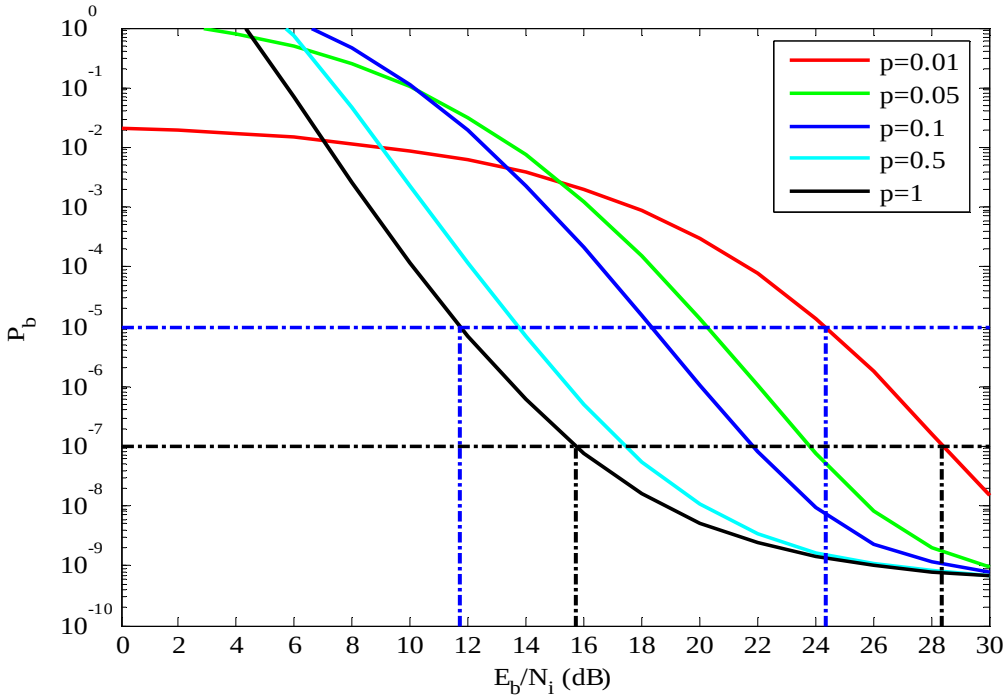

Figure 29. Performance of r=2/3, K=2 convolutional code with 8-BOK, HDD and PNI with E_b/N_o =10.394 dB

The SNR of 10.394 dB is the SNR required for this system to reach $P_b=10^{-9}$ when ρ=1 and SIR=26 dB. It is obvious that as ρ decreases the performance of the system worsens and then improves for the same SIR. Taking as a reference point the probability

of bit error $P_b=10^{-5}$, a degradation of 12.595 dB due to pulse-noise interference is observed. At $P_b=10^{-7}$ the degradation is almost the same, 12.687 dB.

2. Performance of 8-BOK with *r*=2/3 and *K*=3 Convolutional Code in a Pulse-Noise Interference Environment

In Figure 30 the performance of 8-BOK with a $r=2/3$, $K=3$ convolutional encoder in a pulse-noise interference environment is shown.

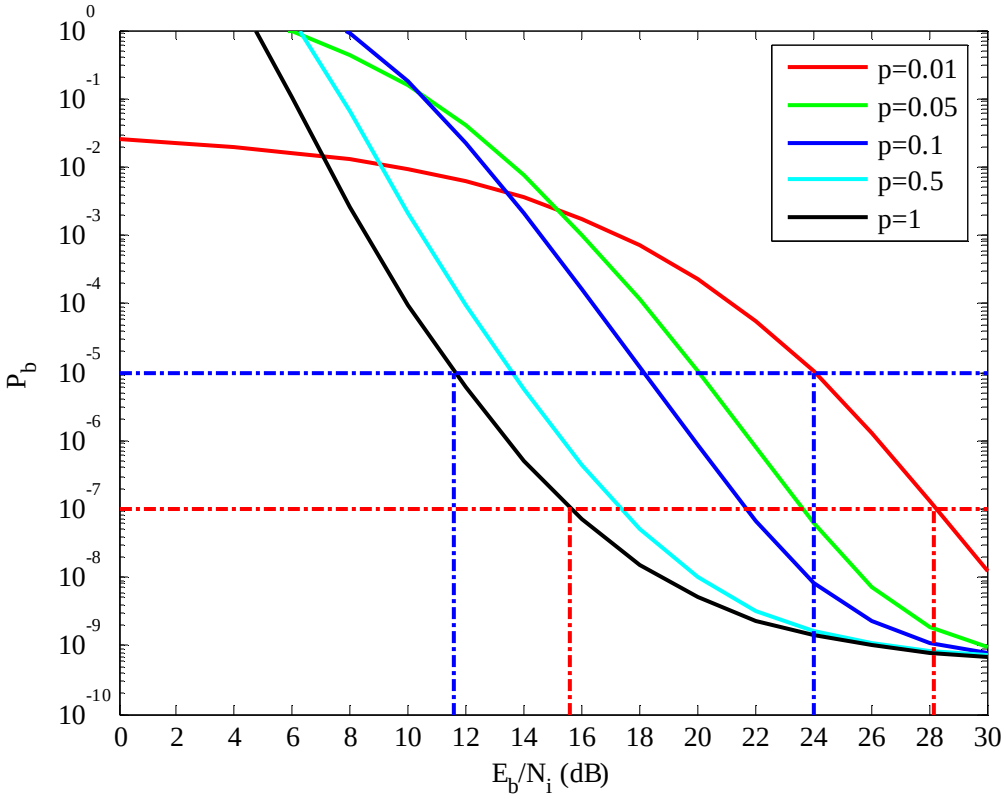

Figure 30. Performance of $r=2/3$, $K=3$ convolutional code with 8-BOK, HDD and PNI with E_b/N_o =10.33 dB

The SNR when $K=3$ is 10.394 dB, a little less than for $K=2$ and is the SNR required for this system to reach $P_b=10^{-9}$ when $\rho=1$ and SIR=26 dB. It is obvious once again that as ρ decreases the performance of the system worsens and then improves for some SNR. At $P_b=10^{-5}$ the degradation of 12.435 dB due to pulse-noise interference is observed, almost the same as with $K=2$. At $P_b=10^{-7}$ the degradation is almost the same, 12.609 dB, as compared with $K=2$. The first conclusion regarding degradation is that an

increase of the encoder memory elements by one does not play an important role in the immunity of the system to pulse-noise interference, which remained almost the same.

3. Performance of 8-BOK with r=2/3 and K=4 Convolutional Code in a Pulse-Noise Interference Environment

In Figure 31 the performance of 8-BOK with a r=2/3, K=4 convolutional encoder in a pulse-noise interference environment is shown.

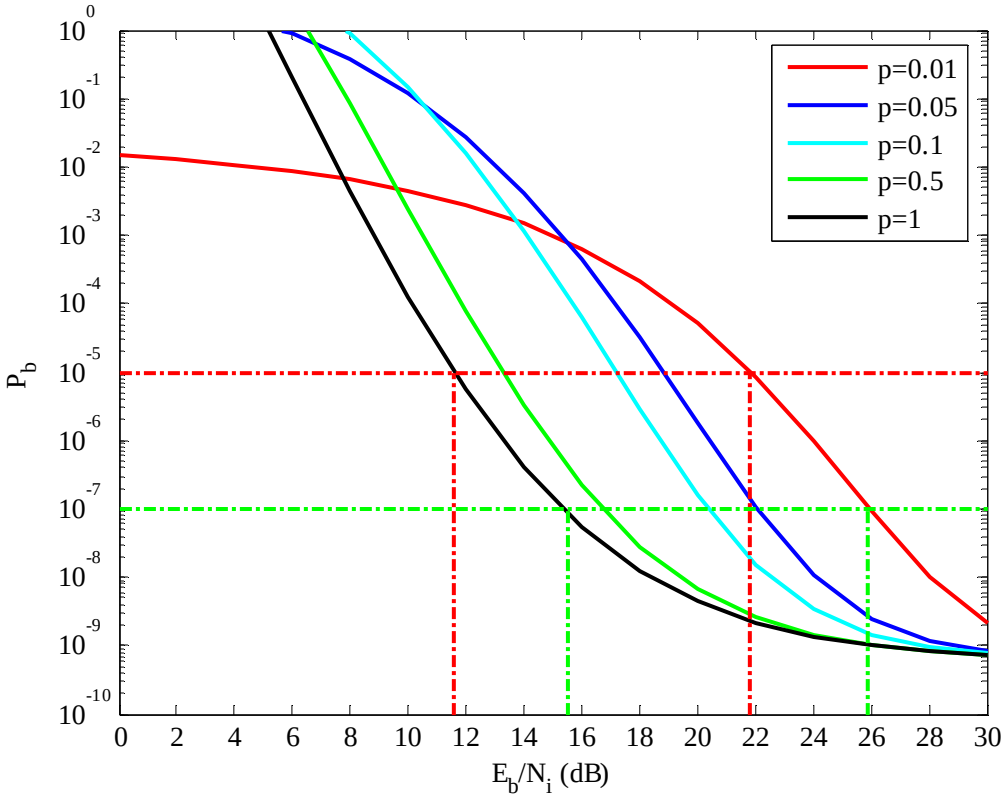

Figure 31. Performance of r=2/3, K=4 convolutional code with 8-BOK, HDD and PNI with E_b/N_o =9.177 dB

The SNR when K=4 is 9.177 dB, almost 1 dB less than that for K=3, and is the SNR required for this system to reach P_b=10^{-9} when ρ=1 and SIR=26 dB. At P_b=10^{-5} the degradation of 10.217 dB due to pulse-noise interference is observed, almost 2.2 dB less than for K=3. At P_b=10^{-7} the degradation due to pulse-noise interference is almost 2 dB less compared with K=3, at the value of 10.568 dB. It is observed that for K=4 the system shows better immunity to pulse-noise interference.

4. Performance of 8-BOK with *r*=2/3 and *K=6* Convolutional Code in a Pulse-Noise Interference Environment

In Figure 32 the performance of 8-BOK with a *r*=2/3, *K=6* convolutional encoder in a pulse-noise interference environment is shown.

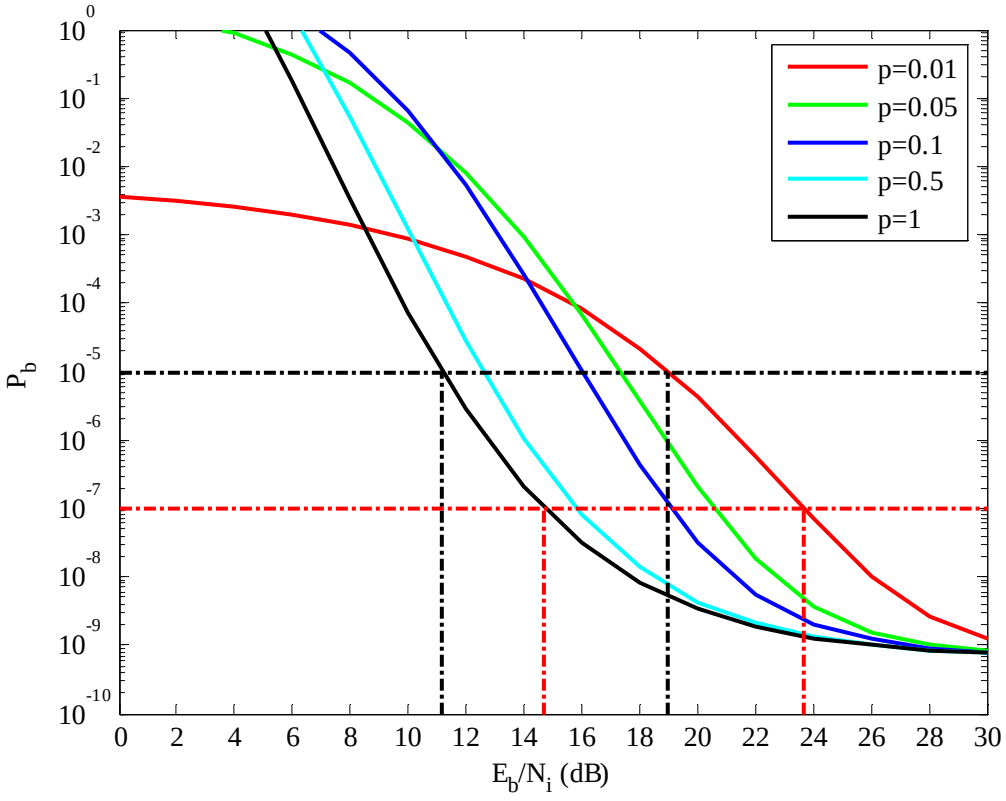

Figure 32. Performance of *r*=2/3, *K*=6 convolutional code with 8-BOK, HDD and PNI with E_b/N_o =8.366 dB

The SNR for *K=6* is 8.366 dB, almost 0.8 dB less than for *K*=4, and is the SNR required for this system to reach $P_b=10^{-9}$ when ρ=1 and SIR=26 dB. At $P_b=10^{-5}$ the degradation of 7.828 dB due to pulse-noise interference is observed, 2.389 dB less than for *K*=4. At $P_b=10^{-7}$ the degradation due to pulse-noise interference is almost 1.6 dB less compared with *K*=4, at 8.967 dB. It is confirmed that as the number of memory elements in the convolutional encoder increases, the better the immunity to pulse-noise interference the system achieves.

5. Comparison of QPSK Modulation with TCM *r*=1/2 and Constraint Length *v*=3 with 8-BOK Modulation *r*=2/3 and *K*=2

In this section a comparison of the TCM system and the 8-BOK system is presented for the same number of memory elements in order to give a better overview of the two systems. The symbol *K* denotes the number of memory elements of the encoder. Many definitions exist for constraint length. The definition of constraint length is not standard, and in this thesis the one used is specified in [8]. The 'constraint length is the maximum number of shifts over which a single *information bit* can affect the encoder output'. Consequently, a *r*=1/2, *v*=3 convolutional encoder has *K*=2.

In Figure 33 the performance of the two systems is shown. The SNR is 8.691 dB and is the required SNR for the TCM system to obtain $P_b = 10^{-9}$ in a continuous interference environment when the SIR is 26 dB. It is obvious that with this SNR the TCM system reaches $P_b=10^{-9}$. On the contrary, the 8-BOK system barely approaches $P_b = 10^{-6}$.

In Figure 33, taking as a reference the performance for $P_b = 10^{-5}$, the comparison between the curves for $\rho=1$ and $\rho=0.1$ for the TCM system yields a difference of 2.858 dB, which can be translated as a degradation of the system due to pulse-noise interference. In contrast the difference between the curves for the 8-BOK system for $\rho=1$ and $\rho=0.01$ at $P_b = 10^{-5}$ yields a difference of 9.375 dB. At $P_b = 10^{-7}$ the TCM system experiences 5.212 dB degradation due to pulse-noise interference. On the contrary, the 8-BOK system does not even reach this probability of bit error for the SNR used. Both systems have in general better performance for the smaller values of ρ. It can be generally said that sometimes, as ρ decreases, the performance worsens but then improves. Finally, it is obvious that even for constraint length *v*=3 the TCM system shows great immunity to pulse-noise interference and experiences 6.517 dB less degradation than the 8-BOK system at $P_b = 10^{-5}$.

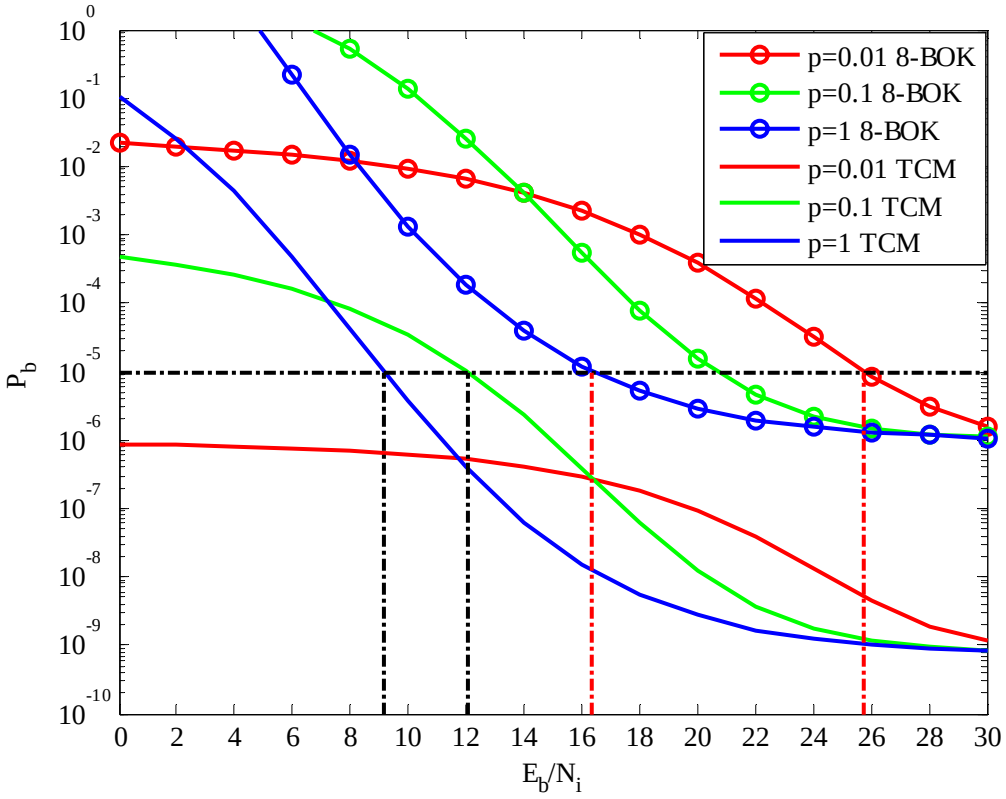

Figure 33. Comparison of r=1/2,v=3 convolutional code with QPSK TCM PNI and r=2/3, K=2 convolutional code with 8-BOK HDD and PNI with E_b/N_o =8.691 dB

6. Comparison of QPSK Modulation with TCM r=1/2 and Constraint Length v=4 with 8-BOK Modulation, r=2/3 and K=3

In Figure 34 the performance of the two systems is shown.

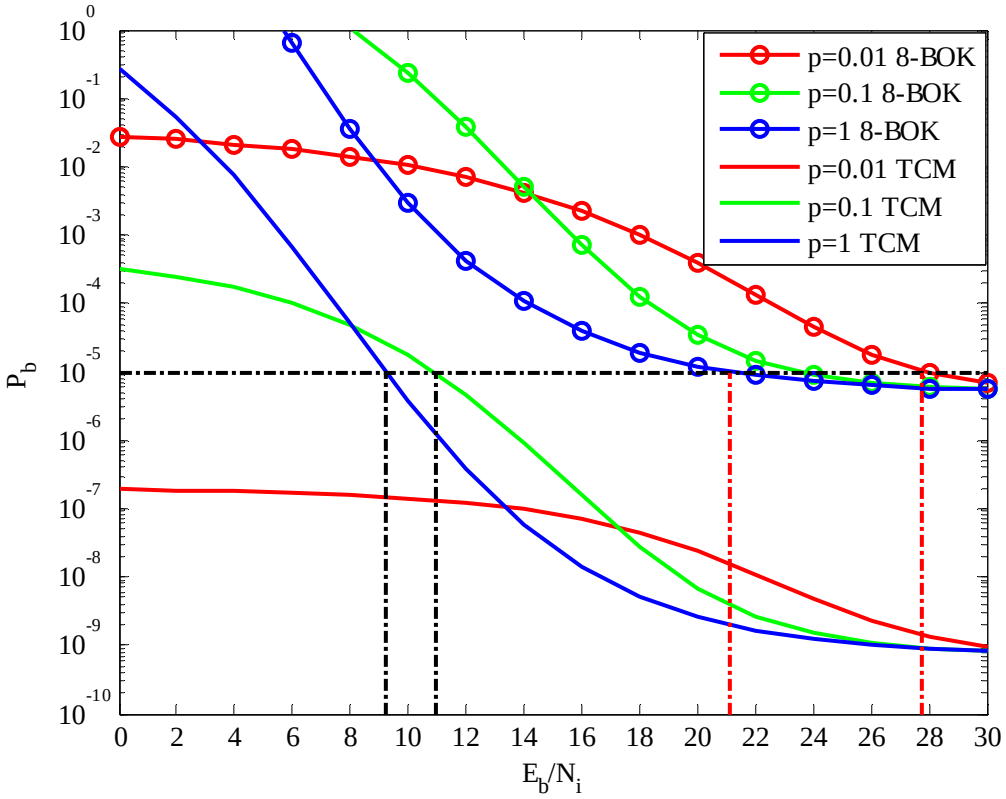

Figure 34. Comparison of r=1/2,v=4 convolutional code with QPSK TCM PNI and r=2/3, K=3 convolutional code with 8-BOK HDD and PNI with E_b/N_o =8.123 dB

The SNR is 8.123 dB and is the SNR required for the TCM system to obtain $P_b = 10^{-9}$ in a continuous interference environment when SIR=26 dB. It is obvious that with this SNR the TCM system reaches $P_b=10^{-9}$. On the contrary, the 8-BOK system barely approaches $Pb=10^{-5}$.

At $P_b = 10^{-5}$, the degradation of the TCM system due to pulse-noise interference is 1.685 dB. In contrast, for the same BER the 8-BOK system experiences 6.647 dB degradation due to pulse-noise interference. At $P_b = 10^{-7}$ the TCM system experiences 1.688 dB degradation due to pulse-noise interference. On the contrary, the 8-BOK system does not even reach this probability of bit error for this SNR. Finally, it is obvious that,

for constraint length v=4, the TCM system shows great immunity to pulse-noise interference and experiences almost 5 dB less degradation than the 8-BOK system at $P_b = 10^{-5}$.

7. Comparison of QPSK Modulation with TCM *r*=1/2 and Constraint Length *v*=5 with 8-BOK Modulation *r*=2/3 and *K*=4

In Figure 35 the performance of the two systems is shown.

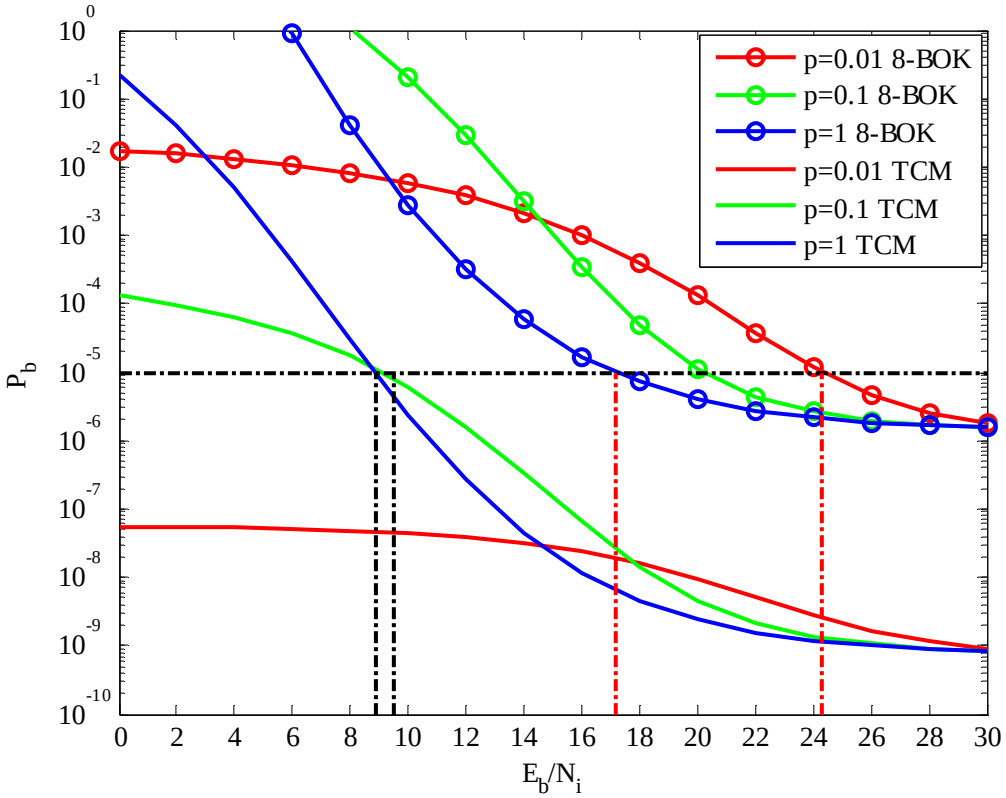

Figure 35. Comparison of r=1/2,v=5 convolutional code with QPSK TCM PNI and r=2/3, K=4 convolutional code with 8-BOK HDD and PNI with E_b/N_o =7.68 dB

The SNR required for the TCM system to obtain $P_b = 10^{-9}$ in a continuous interference environment when SIR=26 dB is 7.68 dB. It is obvious that with this SNR the TCM system reaches P_b=10^{-9}. On the contrary, the 8-BOK system with this SNR does not reach $P_b = 10^{-6}$.

At $P_b = 10^{-5}$, the degradation of the TCM system due to pulse-noise interference is 0.694 dB. In contrast, for the same BER the 8-BOK system experiences 7.134 dB degradation due to pulse-noise interference. At $P_b = 10^{-7}$ the TCM system experiences 2.82 dB degradation due to pulse-noise interference. On the contrary, the 8-BOK system does not even reach this probability of bit error for this SNR. Finally, it is obvious that for constraint length *v=5*, the TCM system shows great immunity to pulse-noise interference and experiences 6.44 dB less degradation than the 8-BOK system at $P_b = 10^{-5}$.

B. PERFORMANCE ANALYSIS OF 16-BOK WITH *R*=3/4 CONVOLUTIONAL ENCODER, IN A PULSE-NOISE INTERFERENCE ENVIRONMENT

The last alternative system to be analyzed and compared with QPSK TCM *r*=1/2 is 16-BOK modulation with *r*=3/4 convolutional encoder. The null-to-null bandwidth for M-BOK is obtained from Equation (3.11) and for 16-BOK, as shown in Equation (3.16), is $BW = 44/24\,R_b$. The bandwidth once again is a little bit less as compared with the bandwidth for the TCM system which is $BW = 2R_b$. For the performance analysis of 16-BOK and for the same reason as has already mentioned for 8-BOK, HDD is used. From Equation (5.4) the probability of channel bit error is obtained. The probability P_d is obtained from Equation (5.5). Finally, from Equation (5.6) the probability of bit error can be evaluated. 16-BOK is used with a code rate *r*=3/4 convolutional encoder in order to meet the bandwidth requirements, and the values of B_d are specified in Table 4 for code rate *r*=3/4 convolutional encoders.

1. Performance of 16-BOK with *r*=3/4 and *K*=2 Convolutional Code in a Pulse-Noise Interference Environment

In Figure 36 the performance of 16-BOK with a *r*=3/4, *K*=2 convolutional encoder in a pulse-noise interference environment is shown. The SNR of 9.25 dB is the required SNR for this system to reach $P_b=10^{-9}$ when $\rho=1$ and SIR=26 dB. This is approximately 1 dB less than the SNR of 8-BOK for the same number of memory elements. It is obvious that as ρ decreases the performance of the system initially worsens and then improves. Taking as a reference point the probability of bit

error $P_b = 10^{-5}$, we observe a degradation of 13.85 dB due to pulse-noise interference, almost 1.2 dB more than 8-BOK. At BER P_b=10^{-7} the degradation remains almost the same at 13.257 dB but is still 0.5 dB more than for 8-BOK.

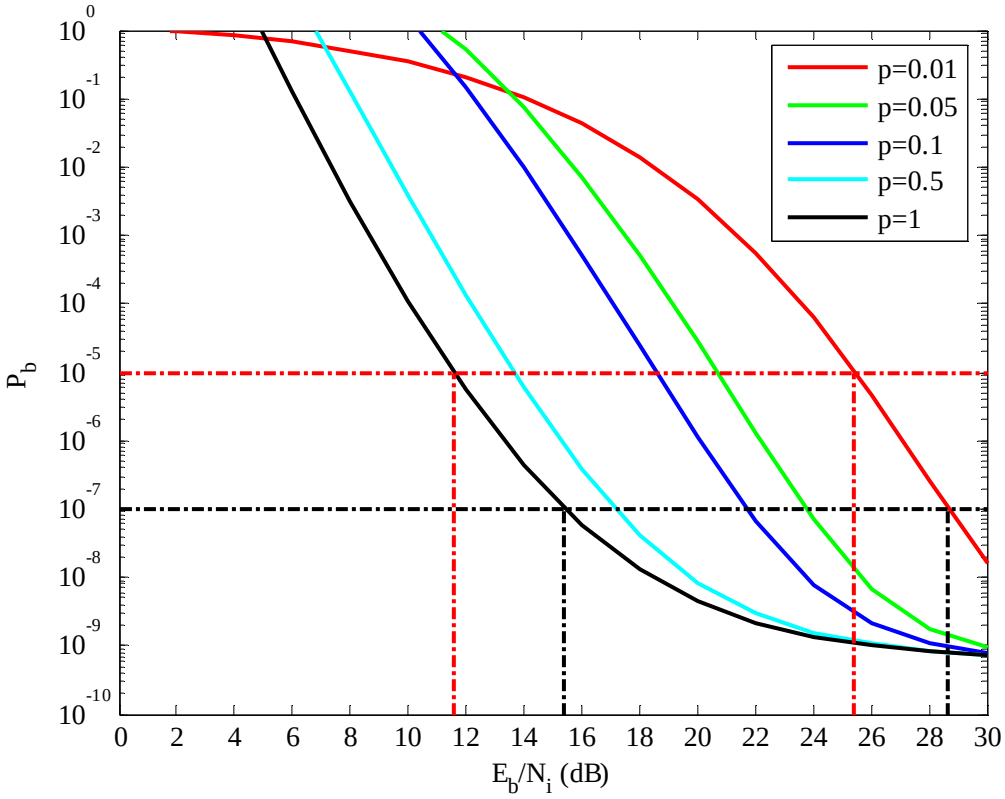

Figure 36. Performance of r=3/4, K=2 convolutional code with 16-BOK, HDD and PNI with E_b/N_o =9.25 dB

2. Performance of 16-BOK with r=3/4 and K=3 Convolutional Code in a Pulse-Noise Interference Environment

In Figure 37 the performance of 16-BOK with a r=3/4, K=3 convolutional encoder in a pulse-noise interference environment is shown. The SNR when K=3 for this system to reach P_b=10^{-9} when ρ=1 and SIR=26 dB, is 9.257 dB, a little bit more than for K=2. The reason has been discussed in detail in Chapter III. Regarding ρ, we see that as ρ decreases the performance of the system initially worsens and then improves. At P_b=10^{-5} a degradation of 13.86 dB due to pulse-noise interference is observed, almost the same as with K=2. At BER P_b=10^{-7} the degradation remains almost the same at 13.264 dB as compared with 16-BOK with K=2. The first conclusion is that an increase of the encoder

memory by one does not play an important role in increasing the immunity of the system to pulse-noise interference, which remained almost the same. Noteworthy is that up to now 16-BOK with r=3/4 convolutional encoding shows less immunity to pulse-noise interference by about 1.2 dB at P_b=10^{-5} and 0.5 dB at P_b=10^{-7} as compared to 8-BOK with r=2/3 convolutional encoding.

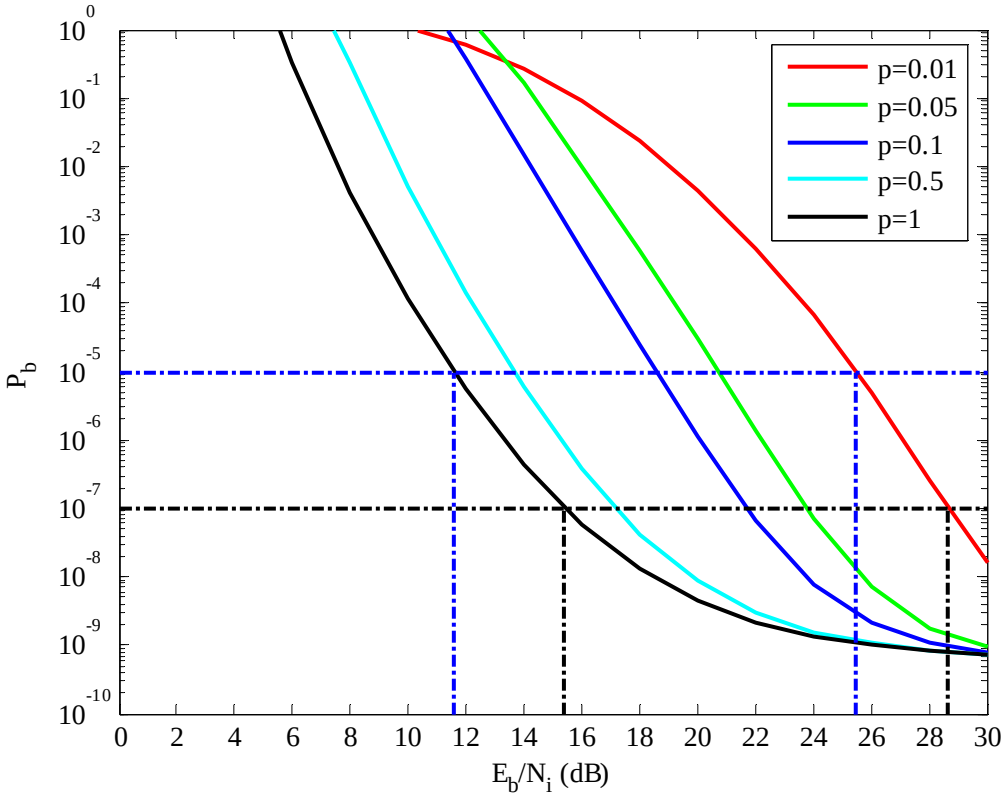

Figure 37. Performance of r=3/4, K=3 convolutional code with 16-BOK, HDD and PNI with E_b/N_o =9.257 dB

3. Performance of 16-BOK with r=3/4 and K=4 Convolutional Code in a Pulse-Noise Interference Environment

In Figure 38 the performance of 16-BOK with a r=3/4, K=4 convolutional encoder in a pulse-noise interference environment is shown. The SNR when K=4 is 8.949 dB and is the required SNR for this system to reach P_b=10^{-9} when ρ=1 and SIR=26 dB. From Figure 38, we reach the same conclusions regarding ρ as for K=3. At P_b=10^{-5} the degradation of 13.34 dB due to pulse-noise interference is observed, almost 0.5 dB less

than for K=3. At P_b=10^{-7} the degradation due to pulse-noise interference is almost 0.3 dB less compared with K=3, at 12.96 dB. It is observed that for K=4 the system shows somewhat larger immunity to pulse-noise interference.

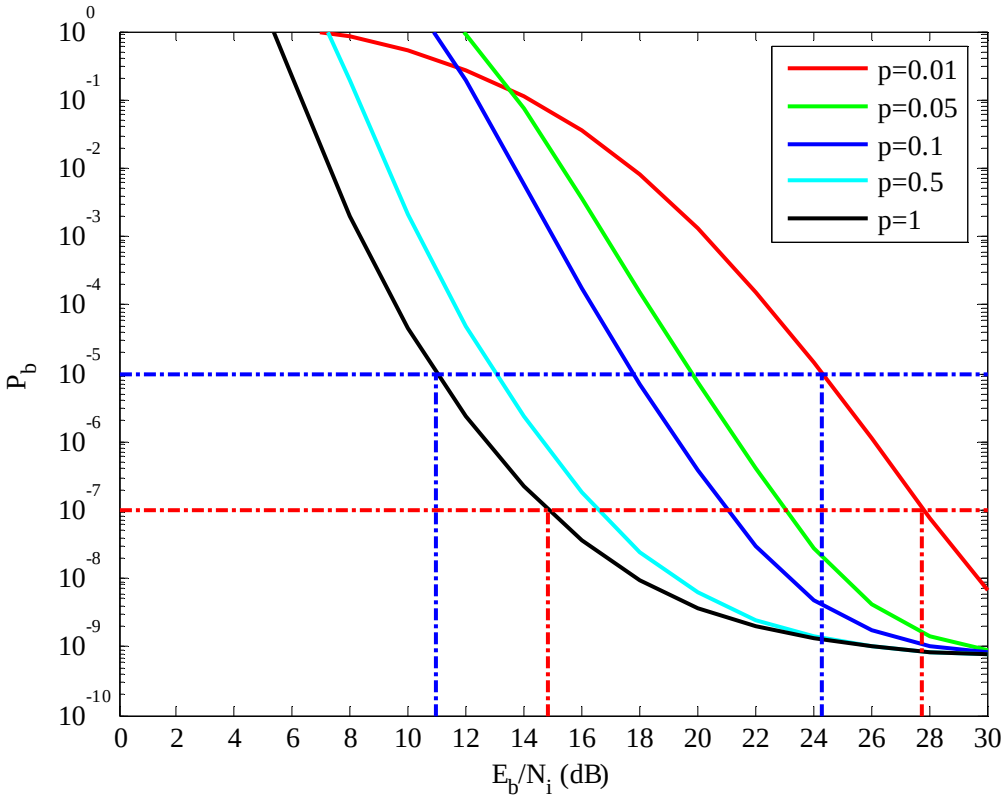

Figure 38. Performance of r=3/4, K=4 convolutional code with 16-BOK, HDD and PNI with E_b/N_o =8.949 dB

4. Performance of 16-BOK with *r*=3/4 and *K=6* Convolutional Code in a Pulse-Noise Interference Environment

In Figure 39 the performance of 16-BOK with a r=3/4, K=6 convolutional encoder in a pulse-noise interference environment is shown. The SNR for K=6 is 7.82 dB, almost 1.1 dB less than for K=4, and is the SNR required for this system to reach P_b=10^{-9} when ρ=1 and SIR=26 dB. From Figure 38, we reach the same conclusions regarding ρ except for ρ=0.01. At P_b=10^{-5} the degradation of 11.417 dB due to pulse-noise interference is observed, almost 2 dB less than for K=4, but 3.589 dB more than 8-BOK. At P_b=10^{-7} the degradation due to pulse-noise interference is almost 1.8 dB less compared with K=4, at 11.078 dB, but 2.1 dB more than for 8-BOK. It can be seen that

as the number of memory elements in the convolutional encoder increases, better immunity to pulse-noise interference is achieved. Also, the performance of the 16-BOK, r=3/4 system is poorer compared with the performance of 8-BOK, r=2/3 for the same number of memory elements.

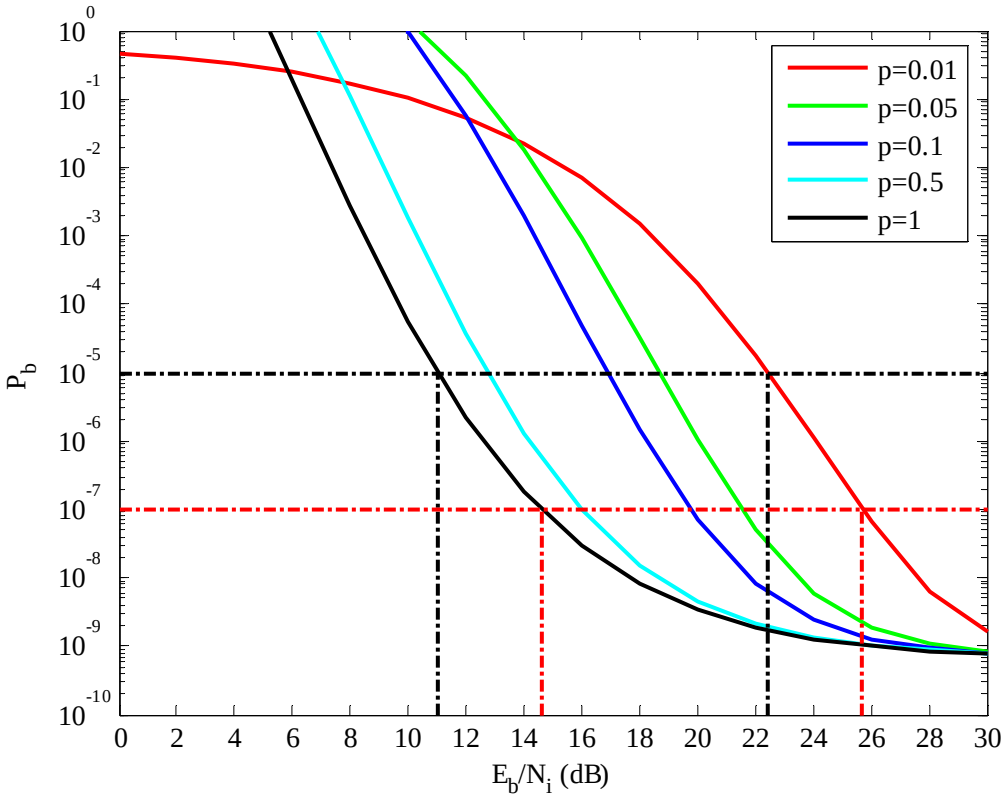

Figure 39. Performance of r=3/4, K=6 convolutional code with 16-BOK, HDD and PNI with E_b/N_o =7.82 dB

5. Comparison of QPSK Modulation with TCM r=1/2 and Constraint Length v=3 with 16-BOK Modulation r=3/4 and K=2

In Figure 40 the performance of the two systems is shown. The SNR of 8.691 dB is the required SNR for the TCM system to obtain $P_b = 10^{-9}$ in a continuous interference environment when the SIR is 26 dB. It is obvious that with this SNR the TCM system reaches P_b=10^{-9}. On the contrary, the 8-BOK system does not reach P_b=10^{-8}.

In Figure 40, taking as a reference the performance for $P_b = 10^{-5}$, the comparison between the curves for ρ=1 and ρ=0.1 for the TCM system yields a difference of 2.858

dB, which can be translated as a degradation of the system due to pulse-noise interference. In contrast, the difference between the plots for the 16-BOK system for ρ=1 and ρ=*0.0*1 at $P_b = 10^{-5}$ yields a difference of 12.99 dB. Both systems have in general better performance for the smaller values of ρ. Generally, it can be said that as ρ decreases the performance worsens but then improves. Finally, it is obvious that even for constraint length v=3 the TCM system shows great immunity to pulse-noise interference and experiences 10.13 dB less degradation than the 16-BOK system at $P_b = 10^{-5}$.

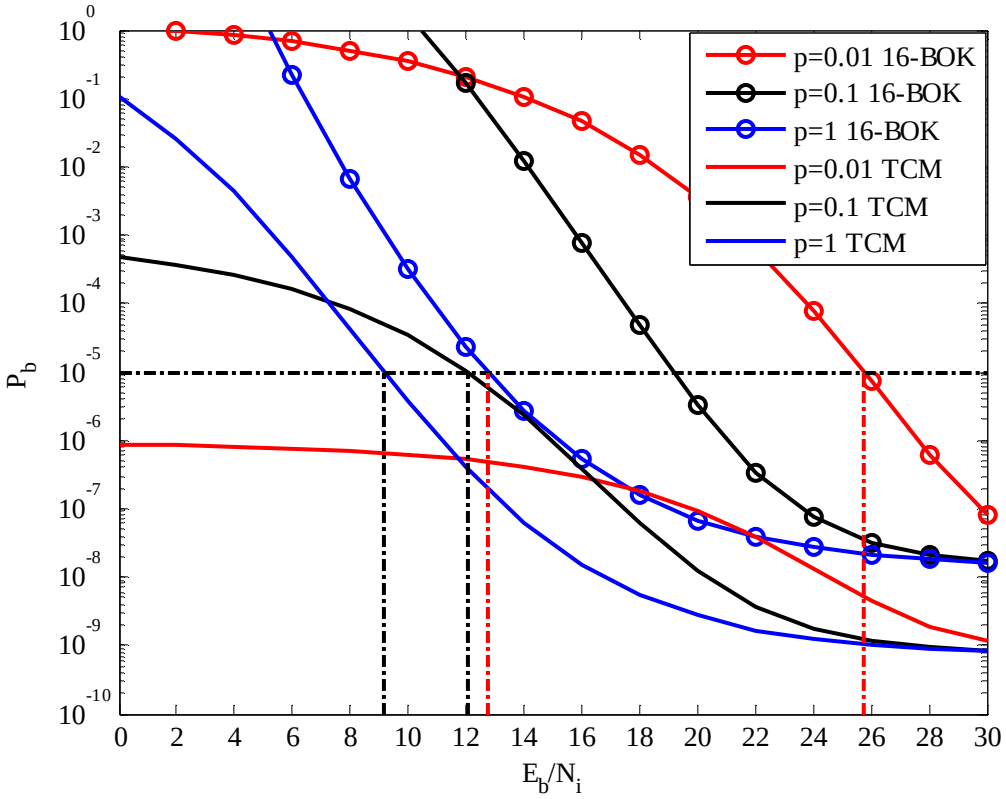

Figure 40. Comparison of r=1/2,v=3 convolutional code with QPSK TCM PNI and r=3/4, K=2 convolutional code with 16-BOK HDD and PNI with E_b/N_o =8.691dB

6. Comparison of QPSK Modulation with TCM *r*=1/2 and Constraint Length *v*=4 with 16-BOK Modulation *r*=3/4 and *K*=3

In Figure 41 the performance of the two systems is shown.

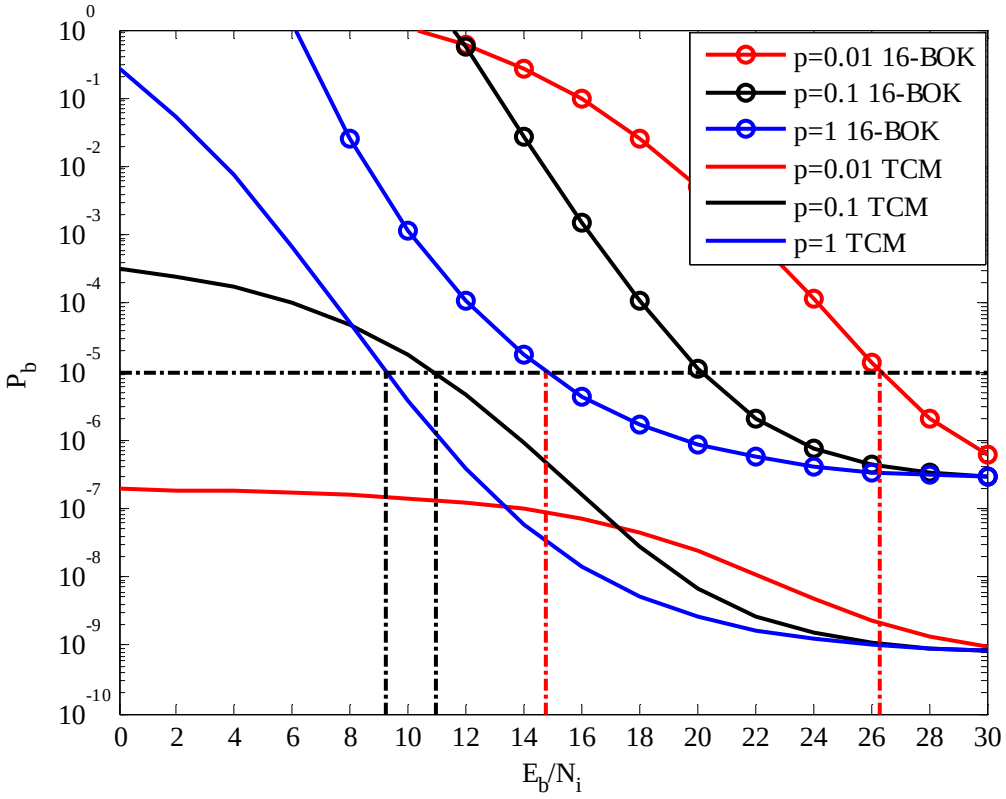

Figure 41. Comparison of r=1/2,v=4 convolutional code with QPSK TCM PNI and r=3/4, K=3 convolutional code with 16-BOK HDD and PNI with E_b/N_o =8.123 dB

The SNR of 8.123 dB is the required SNR for the TCM system to obtain $P_b = 10^{-9}$ in a continuous interference environment when SIR=26 dB. It is obvious that with this SNR the TCM system reaches $P_b = 10^{-9}$. On the contrary, the 16-BOK system does not reach $P_b = 8 \times 10^{-6}$.

At $P_b = 10^{-5}$, the degradation of the TCM system due to pulse-noise interference is 1.685 dB. In contrast, for the same BER the 16-BOK system experiences 11.59 dB degradation due to pulse-noise interference. At $P_b = 10^{-7}$ the TCM system experiences 1.688 dB degradation due to pulse-noise interference. On the contrary, the 16-BOK system does not reach this probability of bit error for this SNR. Finally, it is obvious that,

for constraint length v=4, the TCM system shows great immunity to pulse-noise interference and experiences 9.9 dB less degradation than the 16-BOK system at $P_b = 10^{-5}$.

7. Comparison of QPSK Modulation with TCM *r*=1/2 and Constraint Length *v*=5 with 16-BOK Modulation *r*=3/4 and *K*=4

In Figure 42 the performance of the two systems is shown.

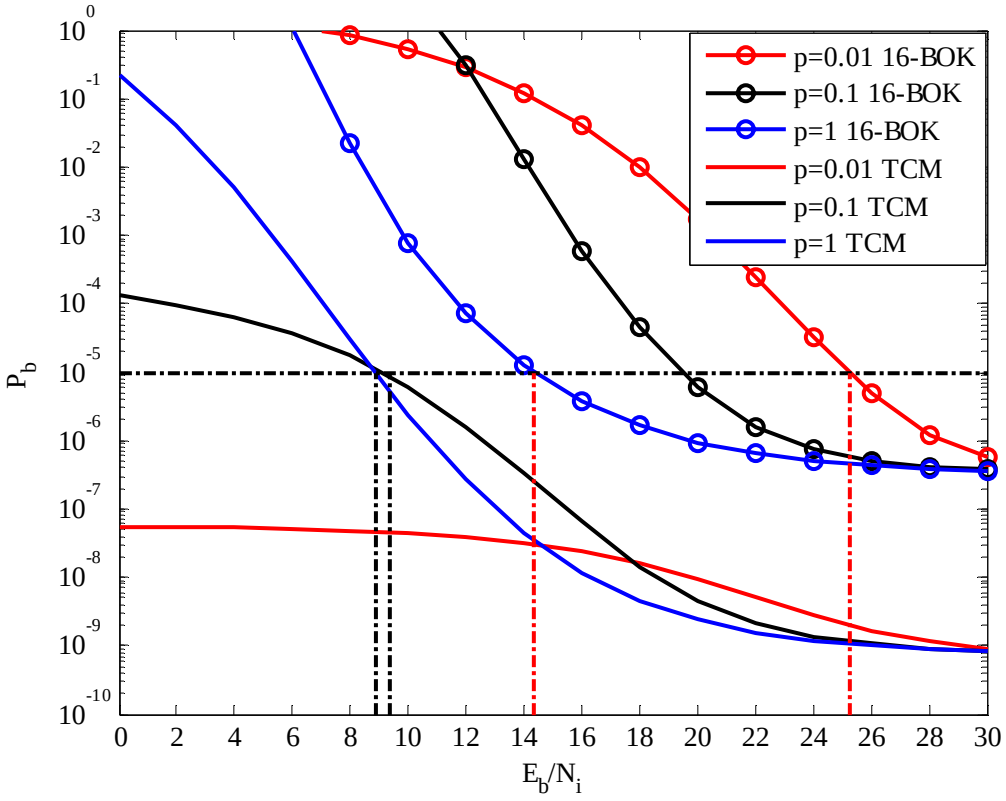

Figure 42. Comparison of r=1/2,v=5 convolutional code with QPSK TCM PNI and r=3/4, K=4 convolutional code with 16-BOK HDD and PNI with E_b/N_o =7.68 dB

The required SNR for the TCM system to obtain $P_b = 10^{-9}$ in a continuous interference environment when SIR=26 dB is 7.68 dB. It is obvious that with this SNR the TCM system reaches P_b=10^{-9}. On the contrary, the 16-BOK system with this SNR does not reach $P_b = 8\times10^{-6}$.

At $P_b = 10^{-5}$, the degradation of the TCM system due to pulse-noise interference is 0.694 dB. In contrast, for the same BER the 16-BOK system experiences 10.894 dB degradation due to pulse-noise interference. At $P_b = 10^{-7}$ the TCM system experiences 2.822 dB degradation due to pulse-noise interference. On the contrary, the 16-BOK system does not reach this probability of bit error for this SNR. Finally, it is obvious that for constraint length v=5 the TCM system shows great immunity to pulse-noise interference and experiences 10.2 dB less degradation than the 16-BOK system at $P_b = 10^{-5}$.

This concludes the TCM system performance analysis in a pulse-noise interference environment and the comparison with 8-BOK with code rate r=2/3 and 16-BOK with code rate r=2/3. In the next and final chapter, we review the results of this thesis with some comments and closing statements.

THIS PAGE INTENTIONALLY LEFT BLANK

VI. CONCLUSIONS

The objective of this thesis was to investigate the performance of a low spectral efficiency TCM system and compare it with several non-TCM systems having comparable spectral efficiencies. The alternative systems were QPSK with independent r=1/2 error correction coding on the in-phase and quadrature components, *8-ary* biorthogonal keying (*8-BOK*) with r=2/3 error correction coding, and 16-BOK with r=3/4 error correction coding. The performance of all systems was analyzed initially given only additive white Gaussian noise (AWGN) and afterwards in a pulse-noise interference (PNI) environment.

A. FINDINGS

1. Conclusions on the Effect of AWGN

The first conclusion comes from Chapter III where only AWGN was considered. The TCM system with QPSK modulation and r=1/2 error correction coding and the non-TCM QPSK with independent r=1/2 error correction coding on the in-phase and quadrature components are shown to have identical performance. On the contrary, the other two alternative systems appear to have poorer performance than the other two, requiring more SNR to achieve the same BER. Moreover, 16-BOK with r=3/4 error correction coding outperforms 8-BOK with r=2/3 error correction coding, requiring a smaller SNR to achieve the same BER.

A second conclusion is that the performance for all of the four systems improves as the number of memory elements in the convolutional encoder increases.

2. Conclusions on the Effect of AWGN plus PNI

In Chapters IV and V the TCM system and the three non-TCM systems were examined in a pulse-noise interference environment for various values of ρ.

The TCM system showed better than expected performance and significant resistance to PNI, and its performance improves as the number of memory element increases. The alternative QPSK system with soft decision decoding (SDD) experienced significant degradation with PNI, showing no immunity at all to pulse-noise interference. On the other hand, 8-BOK with r=2/3 error correction and 16-BOK with r=3/4 error

correction showed better performance in PNI than the alternative QPSK system but worse than the TCM system. It is noteworthy that 16-BOK with r=3/4 error correction coding, which had better performance in AWGN than 8-BOK with r=2/3 error correction coding, in a pulse-noise interference environment showed significant degradation and much worse performance compared with 8-BOK with r=2/3.

Moreover, regarding ρ, the non-TCM systems had in general worse performance for decreasing ρ. On the contrary, the TCM system appeared to have better performance for decreasing ρ.

B. FUTURE WORK

For many years the use of error correction coding in a band limited channel has been of great interest. Ungerboeck, in 1982, showed that coding gains compared with uncoded systems are achievable using the principle of *mapping by set partitioning* without increasing channel bandwidth, and TCM became a great area of interest. In this thesis the system examined was TCM with QPSK modulation and r=1/2 error correction coding up to the constraint length v=5. This thesis constitutes an initial examination of TCM in a pulse-noise interference environment, and to the best of the author's knowledge there has been no related research involving TCM with pulse-noise interference.

The analysis of TCM systems should be extended to larger constraint lengths, although with v=5 sufficient conclusions can be made regarding the performance of the TCM system. Also, the research can be extended to higher code rates such as r=2/3, r=3/4, etc. and M-PSK or M-QAM. Finally, multidimensional TCM or rotationally invariant TCM analysis in a pulse-noise interference environment experiencing fading could be a great area of interest.

C. CLOSING COMMENTS

TCM allows channel coding for band limited systems, such as telephone lines, something which increased robustness or data rates. Many applications use TCM today (ITU V.32 modem standard for 9600 bits/sec, ITU V.33 modem standard for 14400

bits/sec, ITU V-34 modem standard). The examination of TCM in a PNI environment in this thesis may be beneficial to those who are utilizing TCM systems for military applications.

THIS PAGE INTENTIONALLY LEFT BLANK

APPENDIX

In this Appendix, the first two $P_d s$ for the TCM system with rate 1/2, constraint length three, four and five convolutional codes are shown.

For *v*=3, there are two paths with a squared-Euclidean distance of twelve. Hence,

$$P_{12} = P_{12_{(1)}} + P_{12_{(2)}} \tag{A.1}$$

For the first path with $d^2 = 12$

$$P_{12_{(1)}} = E_b\left(\frac{4}{N_1}+\frac{2}{N_2}+\frac{2}{N_3}+\frac{4}{N_4}\right) \tag{A.2}$$

where N_i, *i*=1,2,3,4 are either N_o or N_T. Now

$$\begin{aligned}
P_{12_{(1)}} &= 2(1-\rho)^4 Q\left(\sqrt{\frac{E_b}{N_0}\frac{12}{2}}\right)+ && \text{when } i=0\\
&+\rho(1-\rho)^3\left\{2Q\left(\sqrt{\frac{E_b}{2}\left(\frac{10}{N_0}+\frac{2}{N_T}\right)}\right)+2Q\left(\sqrt{\frac{E_b}{2}\left(\frac{8}{N_0}+\frac{4}{N_T}\right)}\right)\right\}+ && \text{when } i=1\\
&+\rho^2(1-\rho)^2\left\{\begin{array}{l}4Q\left(\sqrt{\frac{E_b}{2}\left(\frac{6}{N_0}+\frac{6}{N_T}\right)}\right)+Q\left(\sqrt{\frac{E_b}{2}\left(\frac{4}{N_0}+\frac{8}{N_T}\right)}\right)\\ +Q\left(\sqrt{\frac{E_b}{2}\left(\frac{8}{N_0}+\frac{4}{N_T}\right)}\right)\end{array}\right\}+ && \text{when } i=2\\
&+\rho^3(1-\rho)\left\{2Q\left(\sqrt{\frac{E_b}{2}\left(\frac{4}{N_0}+\frac{8}{N_T}\right)}\right)+Q\left(\sqrt{\frac{E_b}{2}\left(\frac{2}{N_0}+\frac{10}{N_T}\right)}\right)\right\}+ && \text{when } i=3\\
&+\rho^4 Q\left(\sqrt{\frac{E_b}{N_T}\frac{12}{2}}\right) && \text{when } i=4
\end{aligned} \tag{A.3}$$

Similarly, for the second path with $d^2 = 12$

$$P_{12_{(2)}} = E_b\left(\frac{4}{N_1}+\frac{2}{N_2}+\frac{0}{N_3}+\frac{2}{N_4}+\frac{4}{N_5}\right) \tag{A.4}$$

and

$$
\begin{aligned}
P_{12_{(2)}} = {} & (1-\rho)^5 Q\left(\sqrt{\frac{E_b}{N_0}\frac{12}{2}}\right) + && \text{when } i=0 \\
& +\rho\ (1-\rho)^4 \left\{ \begin{array}{l} 2Q\left(\sqrt{\frac{E_b}{2}\left(\frac{8}{N_0}+\frac{4}{N_T}\right)}\right) + 2Q\left(\sqrt{\frac{E_b}{2}\left(\frac{10}{N_0}+\frac{2}{N_T}\right)}\right) \\ +Q\left(\sqrt{\frac{E_b}{2}\left(\frac{12}{N_0}+\frac{0}{N_T}\right)}\right) \end{array} \right\} + && \text{when } i=1 \\
& +\rho^2(1-\rho)^3 \left\{ \begin{array}{l} 4Q\left(\sqrt{\frac{E_b}{2}\left(\frac{6}{N_0}+\frac{6}{N_T}\right)}\right) + Q\left(\sqrt{\frac{E_b}{2}\left(\frac{4}{N_0}+\frac{8}{N_T}\right)}\right) \\ +3Q\left(\sqrt{\frac{E_b}{2}\left(\frac{8}{N_0}+\frac{4}{N_T}\right)}\right) + 2Q\left(\sqrt{\frac{E_b}{2}\left(\frac{10}{N_0}+\frac{2}{N_T}\right)}\right) \end{array} \right\} + && \text{when } i=2 \\
& +\rho^3(1-\rho)^2 \left\{ \begin{array}{l} 4Q\left(\sqrt{\frac{E_b}{2}\left(\frac{6}{N_0}+\frac{6}{N_T}\right)}\right) + 3Q\left(\sqrt{\frac{E_b}{2}\left(\frac{4}{N_0}+\frac{8}{N_T}\right)}\right) \\ +2Q\left(\sqrt{\frac{E_b}{2}\left(\frac{2}{N_0}+\frac{10}{N_T}\right)}\right) + Q\left(\sqrt{\frac{E_b}{2}\left(\frac{8}{N_0}+\frac{4}{N_T}\right)}\right) \end{array} \right\} + && \text{when } i=3 \\
& +\rho^4(1-\rho) \left\{ \begin{array}{l} 2Q\left(\sqrt{\frac{E_b}{2}\left(\frac{4}{N_0}+\frac{8}{N_T}\right)}\right) + 2Q\left(\sqrt{\frac{E_b}{2}\left(\frac{2}{N_0}+\frac{10}{N_T}\right)}\right) \\ +Q\left(\sqrt{\frac{E_b}{2}\left(\frac{0}{N_0}+\frac{12}{N_T}\right)}\right) \end{array} \right\} + && \text{when } i=4 \\
& +\rho^5 Q\left(\sqrt{\frac{E_b}{N_T}\frac{12}{2}}\right) && \text{when } i=5
\end{aligned}
\qquad \text{(A.5)}
$$

There are four paths with $d^2 = 14$, so

$$P_{14} = P_{14_{(1)}} + P_{14_{(2)}} + P_{14_{(3)}} + P_{14_{(4)}} \tag{A.6}$$

and

$$\begin{aligned}
P_{14_{(1)}} &= E_b\left(\frac{4}{N_1}+\frac{2}{N_2}+\frac{2}{N_3}+\frac{2}{N_4}+\frac{4}{N_5}\right) \\
P_{14_{(2)}} &= E_b\left(\frac{4}{N_1}+\frac{2}{N_2}+\frac{2}{N_3}+\frac{0}{N_4}+\frac{2}{N_5}+\frac{4}{N_6}\right) \\
P_{14_{(3)}} &= E_b\left(\frac{4}{N_1}+\frac{2}{N_2}+\frac{0}{N_3}+\frac{2}{N_4}+\frac{2}{N_5}+\frac{4}{N_6}\right) \\
P_{14_{(4)}} &= E_b\left(\frac{4}{N_1}+\frac{2}{N_2}+\frac{0}{N_3}+\frac{2}{N_4}+\frac{0}{N_5}+\frac{2}{N_6}+\frac{4}{N_7}\right)
\end{aligned} \tag{A.7}$$

For $v = 4$ the probability P_{14} in Equation (4.9) is calculated as follows when pulse-noise interference is present. There are three paths with $d^2 = 14$, so

$$P_{14} = P_{14_{(1)}} + P_{14_{(2)}} + P_{14_{(3)}} \tag{A.8}$$

and

$$\begin{aligned}
P_{14_{(1)}} &= E_b\left(\frac{4}{N_1}+\frac{2}{N_2}+\frac{4}{N_3}+\frac{4}{N_4}\right) \\
P_{14_{(2)}} &= E_b\left(\frac{4}{N_1}+\frac{2}{N_2}+\frac{2}{N_3}+\frac{2}{N_4}+\frac{4}{N_5}\right) \\
P_{14_{(3)}} &= E_b\left(\frac{4}{N_1}+\frac{2}{N_2}+\frac{0}{N_3}+\frac{2}{N_4}+\frac{2}{N_5}+\frac{0}{N_6}+\frac{4}{N_7}\right)
\end{aligned} \tag{A.9}$$

which leads to

$$P_{14_{(1)}} = (1-\rho)^4 Q\left(\sqrt{\frac{E_b}{N_0}\frac{14}{2}}\right) + \quad \text{when } i=0$$

$$+\rho(1-\rho)^3\left\{Q\left(\sqrt{\frac{E_b}{2}\left(\frac{12}{N_0}+\frac{2}{N_T}\right)}\right)+3Q\left(\sqrt{\frac{E_b}{2}\left(\frac{10}{N_0}+\frac{4}{N_T}\right)}\right)\right\}+ \quad \text{when } i=1$$

$$+\rho^2(1-\rho)^2\left\{3Q\left(\sqrt{\frac{E_b}{2}\left(\frac{8}{N_0}+\frac{6}{N_T}\right)}\right)+3Q\left(\sqrt{\frac{E_b}{2}\left(\frac{6}{N_0}+\frac{8}{N_T}\right)+}\right)\right\}+ \quad \text{when } i=2 \qquad \text{(A.10)}$$

$$+\rho^3(1-\rho)\left\{3Q\left(\sqrt{\frac{E_b}{2}\left(\frac{4}{N_0}+\frac{10}{N_T}\right)}\right)+Q\left(\sqrt{\frac{E_b}{2}\left(\frac{2}{N_0}+\frac{12}{N_T}\right)}\right)\right\}+ \quad \text{when } i=3$$

$$+\rho^4 Q\left(\sqrt{\frac{E_b}{N_T}\frac{14}{2}}\right) \quad \text{when } i=4$$

and

$$P_{14_{(2)}} = 2(1-\rho)^5 Q\left(\sqrt{\frac{E_b}{N_0}\frac{14}{2}}\right) + \quad \text{when } i=0$$

$$+\rho\ (1-\rho)^4\left\{2Q\left(\sqrt{\frac{E_b}{2}\left(\frac{10}{N_0}+\frac{4}{N_T}\right)}\right)+3Q\left(\sqrt{\frac{E_b}{2}\left(\frac{12}{N_0}+\frac{2}{N_T}\right)}\right)\right\}+ \quad \text{when } i=1$$

$$+\rho^2(1-\rho)^3\left\{\begin{array}{l}6Q\left(\sqrt{\frac{E_b}{2}\left(\frac{8}{N_0}+\frac{6}{N_T}\right)}\right)+3Q\left(\sqrt{\frac{E_b}{2}\left(\frac{10}{N_0}+\frac{4}{N_T}\right)}\right)\\ +Q\left(\sqrt{\frac{E_b}{2}\left(\frac{6}{N_0}+\frac{8}{N_T}\right)}\right)\end{array}\right\}+ \quad \text{when } i=2$$

$$+\rho^3(1-\rho)^2\left\{\begin{array}{l}6Q\left(\sqrt{\frac{E_b}{2}\left(\frac{6}{N_0}+\frac{8}{N_T}\right)}\right)+3Q\left(\sqrt{\frac{E_b}{2}\left(\frac{4}{N_0}+\frac{10}{N_T}\right)}\right)\\ +Q\left(\sqrt{\frac{E_b}{2}\left(\frac{8}{N_0}+\frac{6}{N_T}\right)}\right)\end{array}\right\}+ \quad \text{when } i=3 \qquad \text{(A.11)}$$

$$+\rho^4(1-\rho)\left\{2Q\left(\sqrt{\frac{E_b}{2}\left(\frac{4}{N_0}+\frac{10}{N_T}\right)}\right)+3Q\left(\sqrt{\frac{E_b}{2}\left(\frac{2}{N_0}+\frac{12}{N_T}\right)}\right)\right\}+ \quad \text{when } i=4$$

$$+\rho^5 Q\left(\sqrt{\frac{E_b}{N_T}\frac{14}{2}}\right) \quad \text{when } i=5$$

For $v=5$, the probability P_{14} in Equation (4.10) is calculated as follows when pulse-noise interference is present. There are two paths with $d^2=14$, so

$$P_{14} = P_{14_{(1)}} + P_{14_{(2)}} \tag{A.12}$$

and

$$P_{14_{(1)}} = E_b\left(\frac{4}{N_1}+\frac{2}{N_2}+\frac{2}{N_3}+\frac{2}{N_4}+\frac{4}{N_5}\right)$$

$$P_{14_{(2)}} = E_b\left(\frac{4}{N_1}+\frac{2}{N_2}+\frac{2}{N_3}+\frac{0}{N_4}+\frac{0}{N_5}+\frac{0}{N_6}+\frac{2}{N_7}+\frac{4}{N_8}\right) \tag{A.13}$$

For $v=5$, the probability P_{16} in Equation (4.10) is calculated as follows when pulse-noise interference is present. There are three paths with $d^2=16$, so

$$P_{16} = P_{16_{(1)}} + P_{16_{(2)}} + P_{16_{(3)}} \tag{A.14}$$

and

$$P_{16_{(1)}} = E_b\left(\frac{4}{N_1}+\frac{2}{N_2}+\frac{0}{N_3}+\frac{4}{N_4}+\frac{2}{N_5}+\frac{4}{N_6}\right)$$

$$P_{16_{(2)}} = E_b\left(\frac{4}{N_1}+\frac{2}{N_2}+\frac{2}{N_3}+\frac{0}{N_4}+\frac{0}{N_5}+\frac{2}{N_6}+\frac{0}{N_7}+\frac{2}{N_8}+\frac{4}{N_9}\right) \tag{A.15}$$

$$P_{16_{(3)}} = E_b\left(\frac{4}{N_1}+\frac{2}{N_2}+\frac{0}{N_3}+\frac{0}{N_4}+\frac{0}{N_5}+\frac{2}{N_6}+\frac{0}{N_7}+\frac{0}{N_8}+\frac{2}{N_9}+\frac{0}{N_{10}}+\frac{2}{N_{11}}+\frac{4}{N_{12}}\right)$$

which leads to

$$
\begin{aligned}
P_{16_{(2)}} = {} & (1-\rho)^6 Q\left(\sqrt{\frac{E_b}{N_0}\frac{16}{2}}\right) + && \text{when } i=0 \\
+\rho\ (1-\rho)^5 & \left\{\begin{array}{l} 3Q\left(\sqrt{\frac{E_b}{2}\left(\frac{12}{N_0}+\frac{4}{N_T}\right)}\right)+2Q\left(\sqrt{\frac{E_b}{2}\left(\frac{14}{N_0}+\frac{2}{N_T}\right)}\right) \\ +Q\left(\sqrt{\frac{E_b}{2}\left(\frac{16}{N_0}+\frac{0}{N_T}\right)}\right) \end{array}\right\} + && \text{when } i=1 \\
+\rho^2(1-\rho)^4 & \left\{\begin{array}{l} 6Q\left(\sqrt{\frac{E_b}{2}\left(\frac{10}{N_0}+\frac{6}{N_T}\right)}\right)+4Q\left(\sqrt{\frac{E_b}{2}\left(\frac{12}{N_0}+\frac{4}{N_T}\right)}\right) \\ +3Q\left(\sqrt{\frac{E_b}{2}\left(\frac{8}{N_0}+\frac{8}{N_T}\right)}\right)+2Q\left(\sqrt{\frac{E_b}{2}\left(\frac{14}{N_0}+\frac{2}{N_T}\right)}\right) \end{array}\right\} + && \text{when } i=2 \\
+\rho^3(1-\rho)^3 & \left\{\begin{array}{l} 6Q\left(\sqrt{\frac{E_b}{2}\left(\frac{10}{N_0}+\frac{6}{N_T}\right)}\right)+6Q\left(\sqrt{\frac{E_b}{2}\left(\frac{6}{N_0}+\frac{10}{N_T}\right)}\right) \\ +7Q\left(\sqrt{\frac{E_b}{2}\left(\frac{8}{N_0}+\frac{8}{N_T}\right)}\right)+Q\left(\sqrt{\frac{E_b}{2}\left(\frac{4}{N_0}+\frac{12}{N_T}\right)}\right) \end{array}\right\} + && \text{when } i=3 \qquad \text{(A.16)} \\
+\rho^4(1-\rho)^2 & \left\{\begin{array}{l} Q\left(\sqrt{\frac{E_b}{2}\left(\frac{2}{N_0}+\frac{14}{N_T}\right)}\right)+6Q\left(\sqrt{\frac{E_b}{2}\left(\frac{6}{N_0}+\frac{10}{N_T}\right)}\right) \\ +3Q\left(\sqrt{\frac{E_b}{2}\left(\frac{8}{N_0}+\frac{8}{N_T}\right)}\right) \end{array}\right\} + && \text{when } i=4 \\
+\rho^5(1-\rho) & \left\{\begin{array}{l} 3Q\left(\sqrt{\frac{E_b}{2}\left(\frac{4}{N_0}+\frac{12}{N_T}\right)}\right)+2Q\left(\sqrt{\frac{E_b}{2}\left(\frac{2}{N_0}+\frac{14}{N_T}\right)}\right) \\ +Q\left(\sqrt{\frac{E_b}{2}\left(\frac{0}{N_0}+\frac{16}{N_T}\right)}\right) \end{array}\right\} + && \text{when } i=5 \\
+\rho^6 Q & \left(\sqrt{\frac{E_b}{N_T}\frac{16}{2}}\right) && \text{when } i=6
\end{aligned}
$$

LIST OF REFERENCES

[1] Ungerboeck, G., "Channel coding with multilevel phase signals" *IEEE Trans. Inform. Theory*, vol. IT-28, pp. 55-67, Jan. 1982.

[2] Proakis, J.G., *Digital Communications*, 4th edition, McGraw Hill, New York, NY, 2001.

[3] Sklar, B., *Digital Communications: Fundamental and Applications*, 2nd edition, Prentice-Hall, Upper Saddle River, NJ, 2001.

[4] Bigliery, Ezio, Divsalar, Dariush, McLane, Peter J. and Simon, Marvin K., *Introduction to Trellis-coded Modulation with applications*, Prentice-Hall, Inc.,May 1991.

[5] Robertson, Clark, Notes for EC4580 (Error Correction Coding), Naval Postgraduate School, Monterey, CA , 2001 (unpublished)

[6] Costello, Daniel J. and Lin, Shu, Error Control Coding: *Fundamental and Applications*., 2nd edition, Prentice-Hall, Upper Saddle River, NJ,2004.

[7] Robertson, Clark, Notes for EC4550 (M-ary Digital Communication Systems), Naval Postgraduate School, Monterey, CA, 2001 (unpublished)

[8] Haykin, S., *Communication Systems*. 3rd edition, John Wiley & Sons, New York, NY, 1994.

THIS PAGE INTENTIONALLY LEFT BLANK

INITIAL DISTRIBUTION LIST

1. Defense Technical Information Center
   Ft. Belvoir, Virginia

2. Dudley Knox Library
   Naval Postgraduate School
   Monterey, California

3. Chairman, Code EC
   Department of Electrical and Computer Engineering
   Monterey, California

4. Chairman, Code IS/Bo
   Department of Electrical and Computer Engineering
   Monterey, California

5. Professor R. Clark Robertson, Code EC/Rc
   Department of Electrical and Computer Engineering
   Monterey, California

6. Professor Tri Ha, Code EC/Ha
   Department of Electrical and Computer Engineering
   Monterey, California

7. Embassy of Greece, Air Attaché
   Washington, DC

8. Konstantinos Pyloudis
   Hellenic Air-Force
   Adrianoupoleos 33
   Papagou, Athens, GREECE
   T.K 156-69